# EEG-BASED BRAIN-COMPUTER INTERFACE USING WAVELET COHERENCE AND GRAPH-THEORETIC METHODS

by

**Sencer Melih Deniz**

B.S., in Electrical & Electronics Engineering, Middle East Technical University, 2001

M.S., in Biomedical Engineering, İstanbul Technical University, 2007

Submitted to the Institute of Biomedical Engineering

in partial fulfillment of the requirements

for the degree of

Doctor

of

Philosophy

Boğaziçi University

2025

# EEG-BASED BRAIN-COMPUTER INTERFACE USING WAVELET COHERENCE AND GRAPH-THEORETIC METHODS

**APPROVED BY:**

Prof. Dr. Ahmet Ademoğlu .....
(Thesis Advisor)

Prof. Dr. Tamer Demiralp .....

Prof. Dr. Burak Güçlü .....

Prof. Dr. Esin Öztürk Işık .....

Prof. Dr. Adil Deniz Duru .....

**DATE OF APPROVAL:** 11 July 2025

# ACKNOWLEDGMENTS

I am profoundly grateful to my supervisor, Prof. Dr. Ahmet Ademoğlu, for her invaluable guidance, steadfast support, and insightful contributions throughout my PhD journey. His wise thoughts during our coffee breaks and science dedication were my inspirations. I am glad to be a member of his research team in Neurosignal Analysis Laboratory.

I extend my sincere thanks to Prof. Dr. Tamer Demiralp for his precious guidance and endless enthusiasm on science and physiology. The time I spent under his guidance in Hulusi Behçet Life Sciences Research Laboratory of İstanbul Medical Faculty contributed much to me and to my thesis with his huge expertise. His deep vision and knowledge in physiology have consistently contributed great value to both my thesis and the broader scientific field.

I would like to express my deepest gratitude to Prof. Dr. Arno Villringer to accept and host me as a visiting researcher at the Department of Neurology at the Max Planck Institute of Human Cognitive and Brain Sciences in Leipzig/Germany. It was also a wonderful period in both my life and research. His insights during our conversations were consistently joyful and intellectually inspiring.

I am deeply grateful to Dr. Vadim Nikulin for welcoming me into his research group, Neural Interactions and Dynamics at the Max Planck Institute for Human Cognitive and Brain Sciences, and generously sharing his time and valuable expertise throughout my work. Being part of such a supportive and stimulating research environment has been truly invaluable to me.

I am grateful to Prof. Dr. Burak Güçlü for his constructive and valuable feedback throughout the progress of my thesis.

I am thankful to Prof. Dr. Esin Öztürk Işık for her contributions during her courses, for agreeing to serve on my thesis committee and for reviewing my thesis.

I am thankful to Prof. Dr. Adil Deniz Duru for his very valuable contribution, help, guidance and positive attitude during my thesis. I would also like to thank to Dr. Dilek Göksel Duru for her support and great friendship.

I would also like to acknowledge my former and current team members and friends, Dr. Hüden Neşe, Dr. Moataz Assem, Dr. Esin Karahan, Pınar Adanalı, Mohammad Alwahid in Neurosignal Analysis Laboratory of Boğaziçi University Biomedical Engineering Institute and Dr. Elif Kurt, Dr. Emel Erdoğdu, Dr. Ani Kıcık, Dr. Ali Bayram in Hulusi Behçet Life Sciences Research Laboratory of İstanbul Medical Faculty for their help, support, friendship, and our time spent together.

I would like to thank the members of the research team in Max Planck Institute for Human Cognitive and Brain Sciences in Leipzig , Dr. Mina Jamshidi, Dr. Elena Cesnaite and Dr. Tilman Stephani, for their warm hospitality and help during my research stay with them.

Finally, I am profoundly grateful to my family for their unwavering love, understanding, endless altruism, boundless patience, and encouragement. I would like to dedicate this thesis to them.

This Ph.D. journey has been as much about personal growth as it has been about academic accomplishment, and I am deeply thankful to everyone who has been part of this transformative experience.

# ACADEMIC ETHICS AND INTEGRITY STATEMENT

I, Sencer Melih Deniz, hereby certify that I am aware of the Academic Ethics and Integrity Policy issued by the Council of Higher Education (YÖK) and I fully acknowledge all the consequences due to its violation by plagiarism or any other way.

Name :

Signature:

Date:

# ABSTRACT

## EEG-BASED BRAIN-COMPUTER INTERFACE USING WAVELET COHERENCE AND GRAPH-THEORETIC METHODS

Emotion and cognition, two fundamental aspects of human mental processes, have traditionally been investigated independently. A comprehensive understanding of human mental functioning requires exploration of emotion and cognition. Among various physiological methods, electroencephalography (EEG), stands out as a reliable, non-invasive tool to evaluate emotional and cognitive processes. Studying neural oscillations across various EEG frequency bands and evaluating event-related potentials (ERPs) helps identifying distinct patterns linked to various emotional and cognitive states. In this thesis, pleasant/unpleasant emotional moods as well as low/high cognitive states were discriminated using graph-theoretic features extracted from spatio-temporal components. Wavelet coherence values corresponding to the N100, N200, and P300 single-trial ERP components were examined across the delta, theta, alpha, and beta frequency bands. Subsequently, graph-theoretic analyses were performed on connectivity matrices constructed from wavelet coherence-based functional networks to obtain several global and local graph metrics. These metrics were employed as features in classification using support vector machines (SVM), k-nearest neighbors (k-NN), and linear discriminant analysis (LDA) to enhance the classification accuracy by leveraging graph-theoretic features. Delta band wavelet coherence based graph features enabled accurate classification using SVM. Pleasant/unpleasant emotional moods and low/high cognitive states were classified with average accuracies of up to 92% and 89%, respectively. These findings emphasize the robustness of the proposed approach, highlighting its potential to improve EEG-based assessment of emotional and cognitive states, while paving the way for future brain–computer interface (BCI) applications.

**Keywords:** EEG, Brain-Computer Interface, Wavelet Coherence, Graph Metrics, Event-Related Potential.

# ÖZET

## DALGACIK UYUMLULUĞU VE ÇİZGE KURAMSAL YÖNTEMLERİ KULLANAN EEG TABANLI BEYİN-BİLGİSAYAR ARAYÜZÜ

İnsanın zihinsel süreçlerinin iki temel bileşeni duygu ve biliş geleneksel olarak bağımsız bir şekilde incelenmiştir. İnsan zihinsel işleyişinin kapsamlı bir şekilde anlaşılması, duygu ve bilişin birlikte incelenmesini gerektirir. Çeşitli fizyolojik yöntemler arasında, elektroensefalografi (EEG), duygusal ve bilişsel süreçleri değerlendirmek için güvenilir ve girişimsel olmayan bir araç olarak öne çıkmaktadır. Farklı EEG frekans bantlarındaki nöral salınımların incelemek ve olaya ilişkin potansiyelleri (OİP) değerlendirmek, farklı duygusal ve bilişsel durumlarla ilişkili özgün desenlerin belirlenmesine yardımcı olur. Bu tezde, hoş/hoş olmayan duygusal haller ve düşük/yüksek bilişsel durumlar, uzaysal-zamansal bileşenlerden elde edilen çizge-teorik özellikleri kullanılarak ayırt edilmiştir. N100, N200 ve P300 tek denemelik OİP bileşenlerine karşılık gelen dalgacık uyumluluk değerleri delta, teta, alfa ve beta frekans bantlarında incelenmiştir. Ardından, dalgacık uyumluluğuna dayalı fonksiyonel ağlardan oluşturulan bağlantı matrisleri üzerinde çizge-teorik analizler yapılarak çeşitli küresel ve yerel çizge metrikleri elde edilmiştir. Bu metrikler, çizge-teorik özniteliklerden yararlanarak sınıflandırma doğruluğunu artırmak amacıyla destek vektör makineleri (SVM), en yakın komşular (k-NN) ve doğrusal ayırt edici analiz (LDA) yöntemleriyle yapılan sınıflandırmada öznitelik olarak kullanılmıştır. Delta bandındaki dalgacık tutarlılığından elde edilen çizge öznitelikleri, SVM yöntemi kullanılarak yüksek doğrulukla sınıflandırma sağlamıştır. Hoş/hoş olmayan duygusal haller ve düşük/yüksek bilişsel durumlar sırasıyla %92 ve %89'a varan ortalama doğruluklarla sınıflandırılmıştır. Bu bulgular, önerilen yaklaşımın gürbüzlüğünü vurgulayarak, duygusal ve bilişsel durumların EEG tabanlı değerlendirmesini geliştirme potansiyelini ortaya koyarken gelecekteki beyin-bilgisayar arayüzü uygulamalarının önünü açmaktadır.

**Anahtar Sözcükler:** EEG, Beyin-Bilgisayar Arayüzü, Dalgacık Uyumluluğu, Çizge Metrikleri, Olaya İlişkin Potansiyel.

# TABLE OF CONTENTS

ACKNOWLEDGMENTS . . . . . iii
ACADEMIC ETHICS AND INTEGRITY STATEMENT . . . . . v
ABSTRACT . . . . . vi
ÖZET . . . . . vii
LIST OF FIGURES . . . . . x
LIST OF TABLES . . . . . xii
LIST OF SYMBOLS . . . . . xiii
LIST OF ABBREVIATIONS . . . . . xiv
1. INTRODUCTION . . . . . 1
1.1 Outline of the Thesis . . . . . 1
1.2 Background . . . . . 2
1.3 Significance of the Study . . . . . 4
1.4 Research Objective . . . . . 5
2. LITERATURE REVIEW . . . . . 6
2.1 Brain-Computer Interfaces . . . . . 6
2.2 Emotional and Cognitive Dynamics in EEG . . . . . 7
2.3 Event-Related Potentials (ERPs) . . . . . 9
2.4 Wavelet Coherence . . . . . 10
2.5 Graph-Based EEG Connectivity . . . . . 12
2.6 Graph Theory in Neuroscience . . . . . 14
3. METHODOLOGY . . . . . 18
3.1 Emotional Data Subjects . . . . . 18
3.2 Emotional Data Acquisition and Experimental Paradigm . . . . . 18
3.3 Cognitive Data Subjects . . . . . 20
3.4 Cognitive Data Acquisition and Experimental Paradigm . . . . . 21
4. EMOTIONAL DATA ANALYSIS AND RESULTS . . . . . 24
4.1 Preprocessing . . . . . 24
4.2 ERP Analysis . . . . . 25
4.3 Wavelet Analysis . . . . . 27

4.4 Wavelet Coherence . . . . . 37
4.5 Graph-Theoretic Metrics . . . . . 40
5. COGNITIVE DATA ANALYSIS AND RESULTS . . . . . 46
5.1 Preprocessing . . . . . 46
5.2 ERP Analysis . . . . . 47
5.3 Wavelet Coherence Analysis . . . . . 49
5.4 Graph-Theoretic Metrics . . . . . 51
6. DISCUSSION . . . . . 54
6.1 Comparison with Existing Literature . . . . . 54
6.2 Summary of Key Findings . . . . . 55
7. CONCLUSION . . . . . 58
7.1 Limitations of the Study . . . . . 58
7.2 Future Directions . . . . . 59
7.3 Proceedings and Articles During Thesis . . . . . 59
Bibliography . . . . . 61

# LIST OF FIGURES


| | | |
|---|---|---|
| Figure 1.1 | A typical BCI system with several types of feedback. | 3 |
| Figure 2.1 | Adjacency matrix shown conceptually. | 14 |
| Figure 2.2 | Adjacency matrix shown in weighted matrix notation. | 14 |
| Figure 3.1 | Stimuli durations. | 19 |
| Figure 3.2 | Pleasant (left) and unpleasant (right) images [74]. | 19 |
| Figure 3.3 | Emotional stimuli. | 20 |
| Figure 3.4 | Cognitive paradigm [98]. | 21 |
| Figure 3.5 | Memory stimuli experiment timing. | 23 |
| Figure 4.1 | ERP waveform of F3 channel. | 26 |
| Figure 4.2 | ERP waveform of F4 channel. | 26 |
| Figure 4.3 | ERP waveform of Fz channel. | 26 |
| Figure 4.4 | ERP waveform of Cz channel. | 26 |
| Figure 4.5 | k-NN classification results. | 29 |
| Figure 4.6 | LDA classification results. | 29 |
| Figure 4.7 | SVM classification results. | 30 |
| Figure 4.8 | k-NN classification results. | 31 |
| Figure 4.9 | LDA classification results. | 31 |
| Figure 4.10 | SVM classification results. | 32 |
| Figure 4.11 | k-NN classification results. | 32 |
| Figure 4.12 | LDA classification results. | 33 |
| Figure 4.13 | SVM classification results. | 34 |
| Figure 4.14 | k-NN classification results. | 34 |
| Figure 4.15 | LDA classification results. | 35 |
| Figure 4.16 | SVM classification results. | 36 |
| Figure 4.17 | N100 connectivity maps of difference for delta, theta, alpha, and beta frequency bands. | 38 |
| Figure 4.18 | N200 connectivity maps of difference for delta, theta, alpha, and beta frequency bands. | 39 |

| | | |
|---|---|---|
| Figure 4.19 | P300 connectivity maps of difference for delta, theta, alpha, and beta frequency bands. | 39 |
| Figure 4.20 | Graph measures based classification pipeline. | 43 |
| Figure 5.1 | ERP waveform of F3 channel. | 48 |
| Figure 5.2 | ERP waveform of F4 channel. | 48 |
| Figure 5.3 | ERP waveform of Fz channel. | 48 |
| Figure 5.4 | ERP waveform of C3 channel. | 48 |
| Figure 5.5 | ERP waveform of Cz channel. | 48 |
| Figure 5.6 | ERP waveform of Pz channel. | 48 |
| Figure 5.7 | N100 connectivity maps of difference for delta, theta, alpha, and beta frequency bands. | 49 |
| Figure 5.8 | N200 connectivity maps of difference for delta, theta, alpha, and beta frequency bands. | 50 |
| Figure 5.9 | P300 connectivity maps of difference for delta, theta, alpha, and beta frequency bands. | 51 |

# LIST OF TABLES


| | | |
|---|---|---|
| Table 4.1 | Classification performance for each subject by using energy of N200 and P300 beta wavelet coefficients. | 36 |
| Table 4.2 | SVM classification performance for each subject by using N100, N200, and P300 delta band graph features selected with the *t*-test method. | 44 |
| Table 4.3 | SVM classification performance for each subject by using N100, N200, and P300 delta band graph features selected with the ReliefF method. | 45 |
| Table 5.1 | SVM classification performance for each subject by using N100, N200, and P300 delta band graph features selected with the *t*-test method. | 52 |
| Table 5.2 | SVM classification performance for each subject by using N100, N200, and P300 delta band graph features selected with the ReliefF method. | 53 |

# LIST OF SYMBOLS

| | |
|---|---|
| A | Adjacency matrix |
| $c$ | Number of integration cycle |
| $CC$ | Clustering coefficient of the graph |
| $CPL$ | Characteristic path length of the graph |
| $d_n$ | The degree of node $n$ |
| $d_{xy}$ | Shortest path between the nodes $x$ and $y$ of the directed |
| $\delta$ | Range of integration |
| $Eff$ | Efficiency of the graph |
| $Eng$ | Energy of the graph |
| $f$ | Frequency |
| $\lambda$ | Eigenvalue |
| $\mu$ | Micro |
| $\Omega$ | Ohm |
| $Str_a$ | Strength of node $a$ |
| $t$ | Time |
| $t_n$ | The number of triangles that include node $n$ |
| $Trs$ | Transitivity of the graph |
| $x(t)$ | Time-domain signal $x$ |
| $V$ | The set of all nodes in the graph |
| $W_{ij}$ | Weight of the directed edge from node $i$ to $j$ |
| $W_{xx}(t, f)$ | Wavelet auto-spectrum |
| $W_{xy}(t, f)$ | Wavelet cross-spectrum |
| $WCoh_{xy}(t, f)$ | Wavelet coherence |

# LIST OF ABBREVIATIONS

| | |
|---|---|
| 2D | Two Dimensional |
| AgCl | Silver chloride |
| BCI | Brain-Computer Interface |
| DWT | Continuous Wavelet Transform |
| DT | Deep Target |
| DTI | Diffusion Tensor Imaging |
| DWT | Discrete Wavelet Transform |
| ECG | Electrocardiogram |
| EEG | Electroencephalography |
| EMG | Electromyography |
| EOG | Electroculogram |
| ERP | Event Related Potential |
| fMRI | Functional Magnetic Resonance Imaging |
| GmbH | Gesellschaft mit beschränkter Haftung |
| Hz | Herthz |
| IAPS | International Affective Picture System |
| ICA | Independent Component Analysis |
| k-NN | k-nearest Neighbors |
| LDA | Linear Discriminant Analysis |
| m | Meter |
| MEG | Magnetoencephalography |
| NT | Non-Target |
| PET | Positron Emission Tomography |
| s | Second |
| ST | Shallow Target |
| SVM | Support Vector Machines |

# 1. INTRODUCTION

## 1.1 Outline of the Thesis

This dissertation is structured into the following sections.

Chapter 1 presents a background information and basic principles underlying brain–computer interface systems in addition to research objective and significance of the study.

Chapter 2 provides a brief overview of existing analysis methods, including a literature review of data analysis techniques relevant to the thesis topics.

Chapter 3 details the study's methodology, including data acquisition steps, and experimental paradigms for both emotional and cognitive datasets.

Chapter 4 addresses the preprocessing pipeline and analytical techniques applied to the emotional data, followed by descriptions of the feature extraction and feature selection procedures and obtained results.

Chapter 5 parallels Chapter 4, applying the same analytical framework to the cognitive dataset.

Chapter 6 discusses the comparison with the existing literature and summarizes the key findings of the study.

Chapter 7 covers the study's limitations, proposes directions for future research, and presents a list of publications generated throughout the thesis.

## 1.2 Background

Emotions fundamentally shape our interaction with the environment. Emotional states conveyed through facial expressions, vocal intonation, and body posture form the foundation for meaningful social interactions. Recent studies demonstrate that emotions and motivational contexts significantly impact cognitive processes once considered purely rational, such as perception, attention, memory, and decision-making, thereby challenging the long-held assumption that these functions remain uninfluenced by affective factors [27]. Motivated attention denotes the preferential allocation of attentional resources toward emotionally significant stimuli. Through this mechanism, motivational systems influence cognitive processing, either enhancing or impairing memory, perceptual discrimination, detailed analysis, and readiness for action [18],[75],[113].

The field of cognitive neuroscience is rich in electrophysiological and neuroimaging studies employing rigorous experimental designs to explore fundamental cognitive processes such as decision-making, memory, and attention. In contrast, research focused specifically on the neurophysiological assessment of emotions is comparatively recent and less conclusive. Electroencephalography (EEG) is widely used non-invasive electrophysiological technique to monitor electrical activity in the brain and plays a major role in evaluating motor functions, cognitive workloads, attentional level, and brain and sleep disorders, as well as emotional evaluation [86]. The increasing demand for efficient and reliable methods for human-computer interaction emphasizes the importance of automatic emotion recognition, which plays a crucial role in human communication and strongly influences various cognitive domains [121],[43]. Furthermore, emotion recognition is a critical and essential step of EEG-based brain–computer interfaces (BCIs) designed to support caregiving applications. Therefore, there is a growing interest in the development of affective BCI systems that can accurately interpret and respond to users' emotional states.

Fundamentally, BCI systems utilize EEG signals to execute specific functions and to control external devices, as shown in Figure 1.1. In addition to different categorization, BCI systems are generally classified by two different paradigms:

- *Active BCI :* Active BCI paradigms require users to perform prescribed mental tasks or to respond to externally presented stimuli, thereby producing intentionally modulated neural activity from which the system translates into control commands under conscious and voluntary control. On the contrary, passive BCI paradigms operate in the background, continuously analyzing spontaneous brain activity in the background to deduce the affective or cognitive state of the user without requiring any deliberate effort [150]. Passive BCI paradigms expand BCI technology beyond assistive applications for individuals with disabilities to mainstream human–computer interaction. By non-intrusively monitoring users' ongoing neural activity, they provide an implicit supplementary input channel that complements conventional interaction modalities.

- *Passive BCI :* Passive BCIs enable the simultaneous monitoring of multiple cognitive variables without requiring conscious user involvement. This functionality permits access to a broad range of cognitive states and processes, including underlying mental states such as arousal, fatigue, vigilance, and cognitive workload, as well as transient cognitive events like attention, decision-making and memory encoding [21],[23],[51],[116].

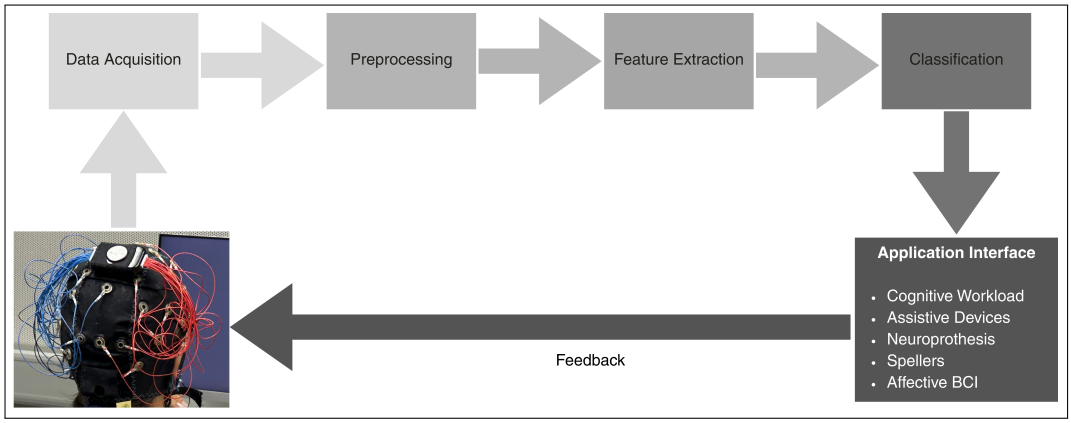


**Figure 1.1** A typical BCI system with several types of feedback.

## 1.3 Significance of the Study

Although some studies examine only cognitive data for analysis, some research focuses on emotional data [80]. Several studies investigate the utility of brain network metrics for emotion recognition [76]. Feature extraction methods include time-domain [105],[73], frequency-domain [141], and time frequency-domain [120],[92] techniques. One of the studies [110] applies the graph theory based method to investigate the cognitive process of emotion, whereas the majority of studies construct connectivity networks using phase-locking value (PLV) [49],[142] or mutual information [148]. On the other hand, event-related potential (ERP) components are used as time domain features [101],[15],[44]. However, these studies do not incorporate wavelet coherence into a graph-theoretic framework and analyze the ERP components as a whole. In addition, there is a lack of established benchmarks for a single pipeline that concurrently addresses emotional and cognitive paradigms. In this context, this thesis fills these gaps by adopting a graph-theoretic approach that utilizes wavelet coherence-based connectivity patterns of various ERP components in both emotional and cognitive settings.

EEG data are collected from 13 subjects as they view images selected to stimuli pleasant or unpleasant emotions for the emotional dataset. The investigation focuses on identifying discriminative features that separate these two emotional moods. Using single-trial data, the N100, N200, and P300 ERP components provide the temporal components, enabling the identification of connectivity patterns that discriminate the two emotional moods. In the cognitive arm of the study, EEG data obtained from 15 subjects are evaluated to determine whether distinct two levels of cognitive load can be reliably differentiated by applying graph-theoretic features derived from spatio-temporal components. In this thesis, emotional and cognitive EEG datasets are analyzed independently.

The aim of this thesis is to identify graph-theoretic metrics based features to provide reliable classification of emotional moods as well as cognitive states. Single-trial ERPs, specifically the N100, N200, and P300 components, are analyzed to distinguish between pleasant and unpleasant stimuli in the emotional data, and between low and

high cognitive states in the cognitive data. This thesis systematically evaluates the feasibility of using these ERP components as features in EEG-based BCI applications across both emotional and cognitive paradigms. This thesis reports the classification results obtained from EEG recordings acquired while subjects participated in rigorously designed paradigms.

## 1.4 Research Objective

As a novel approach, this thesis introduces an innovative analytical pipeline that extracts graph-theoretic metrics from connectivity matrices generated through wavelet coherence analysis of single-trial N100, N200, and P300 ERP components. During this process, each of the delta, theta, alpha, and beta frequency bands is considered individually. The resulting graph metrics constitute feature vectors for conventional machine-learning based classifiers and are evaluated on both emotional and cognitive EEG datasets, enabling discrimination between pleasant and unpleasant emotional moods, as well as between low and high cognitive states.

# 2. LITERATURE REVIEW

This chapter presents a comprehensive review of the relevant literature, examines current investigations pertinent to the thesis topic, and outlines the methodological approaches adopted.

## 2.1 Brain-Computer Interfaces

EEG-based BCI systems to recognize emotions are one of the trending topics with diverse interdisciplinary applications, especially among neuroscientists, because such kind of systems are important for certain use cases [77] such as cognitive workload estimation [71],[149], fatigue detection during driving [118], emotion recognition [82][84],[12],[10] and working memory capacity [35]. Different approaches are applied to monitor these concepts. Various methods, including self-report, startle response, behavioral responses, autonomic measurements, audio-visual expressions, gestures, and neurophysiological assessments, are utilized for emotion recognition [129]. However, audio-visual expressions and gestures are influenced by personal habits shaped by different cultural and language backgrounds. In contrast, physiological signals particularly electroencephalography (EEG), electrocardiogram (ECG), and electromyography (EMG) provide more objective and reliable results to capture emotional and cognitive components[77]. Electrophysiological techniques ensure the most direct access to the brain's primary structures which results in permitting the detection of a broad range of emotional state dynamics [66]. Therefore, they provide the most direct tool for emotion recognition. Although there are other modalities to measure brain activity including functional magnetic resonance imaging (fMRI), magnetoencephalography (MEG), positron emission tomography (PET), and diffusion tensor imaging (DTI), EEG remains widely used in emotion recognition research due to several advantages. First, EEG is non-invasive, portable, and relatively inexpensive hardware [156]. Moreover, EEG provides high temporal resolution, making it ideal for analyzing quick fluctuations in brain activity. The safe and procedurally simple acquisition of EEG data makes

it suitable for almost all populations, including individuals with severe disabilities or paralysis [91],[128].

## 2.2 Emotional and Cognitive Dynamics in EEG

An emotional state space can be built from either the discrete or the dimensional model in the psychological aspects according to research on the structure and functions of emotions [23]. According to the discrete model, emotional state can be described as a combination of discrete states corresponding to one of the core emotions such as anger, fear, disgust, surprise, happiness, and sadness, or a combination of them. Regarding the dimensional model, an emotional state can be described as spatially in valence and arousal dimensions and emotion can be explained through these dimensions. The intensity of the emotive orientation is ruled by arousal, whereas the emotive direction is ruled by valence [55]. Based on these emotion models, neurophysiological mechanisms under the emotional state are widely inquired. Frontal EEG asymmetry, for instance, is consistently linked to the subjective experience of positive versus negative emotions [28]. Recently, affective computing is a major research area in psychological and psychiatric research, supporting assessments of individuals with emotion-related and other neurological disorders alongside healthy populations. It now represents a convergent technological field that integrates emotional processing into BCI-based systems [106]. Emotion recognition, which is the estimation of the emotional state of users from their behavioral and physiological responses, aims enhancing human–computer interaction to create affective user interfaces for healthy people as well as improving psychiatric assessment and intervention. Emotional states play an important role in decision-making and affect problem-solving abilities. Emotional intelligence, which increases professional and personal success, can be improved by emotion recognition [37]. Emotion, personality, and motivation are related with decision-making which is a complex cognitive process [22],[107],[119].

Cognitive workload is a fundamental concept for assessing and monitoring human performance during cognitively demanding tasks [26]. It defines the mental effort

or attentional resources required to perform a task [62]. The cognitive state represents the degree of cognitive workload required by a given task. A low cognitive state denotes negligible demands on processing resources, whereas a high cognitive state indicates that considerable cognitive resources must be deployed to fulfill task requirements. Furthermore, mental health and cognitive workload can be optimized through emotional self-awareness [130]. Measurement of the change in cognitive workload of users is receiving an increasing amount of attention owing to recent advances in wearable and non-invasive electrophysiological technologies [89]. Physiological signals enable the monitoring of key cognitive operations, such as memory, attention, language, problem-solving, and planning, thereby enhancing evaluations in human-machine interaction systems. The literature indicates that EEG-based cognitive workload measurement is employed across a wide range of operational contexts: air traffic management task [6],[34]; optimization of workplace conditions and in-situ assessment of office workers' cognitive states [19],[135]; and assessments of working-memory evaluation during n-back paradigms [88],[104],[140]. Collectively, these studies demonstrate that the classification of diverse cognitive tasks are investigated extensively [47],[63],[81],[87],[152].

Modern psychological science does not view cognition and affect as separable and it is believed that they interact [36]. Research shows that emotional states influence core cognitive operations including attention, memory, and decision-making [43],[121]. Consequently, the simultaneous acquisition of emotional and cognitive data in EEG studies is gaining prominence as a core topic in the multiple fields, particularly within the BCI domain. Due to its high temporal resolution, EEG permits researchers to observe real-time brain activity associated with emotional or cognitive functions. Concurrent monitoring of both data types allows researchers to characterize how emotional states impact cognitive performance during BCI tasks. Therefore, exploiting both data types paves the way for BCIs that respond more effectively to users' mental states, enhancing its robustness and usability. In conclusion, it can be stated that analyzing integrated emotional and cognitive EEG data is crucial for deepening our insight into neural mechanisms and, consequently, for improving BCI technology. For real-world BCI deployment, simultaneous monitoring of both data types should be considered essential. This thesis benchmarks the proposed methodology on two paradigms, namely

emotional and cognitive, without inferring causality between them. Such an integrative framework, especially on rapidly evolving wearable EEG platforms, represents a promising area for future research of next generation and user-centered BCIs.

## 2.3 Event-Related Potentials (ERPs)

In this thesis, both emotional moods and cognitive states are studied by analyzing single-trial EEG signals, from which ERPs are identified. EEG signal can be investigated in the time domain, in the frequency domain, or in a combination of both. In the time domain, ERPs are typically inspected by evaluating the amplitudes and latencies of significant peaks in the grand-averaged waveform [9],[66]. As an example in frequency domain analysis, the Fourier transform provides stationary spectral content but does not give information about the timing of transient neural events [31],[33]. Accordingly, time–frequency analysis of signal is preferred to circumvent these limitations of single-domain methods [33]. Due to such kind of constraints of single-domain analysis [31],[33], it is generally advantageous to employ wavelet transform based signal processing, providing spatio-temporal information, for decomposing EEG signals into oscillatory components across multiple frequency bands [13].

In order to classify tasks such as imagery, actual movement, and cursor control, either a single trial or an average of a few trials can be utilized. On the other hand, some BCIs require multiple trials to be averaged following specific stimulus presentations [89]. Nonetheless, averaging EEG results across multiple subjects and trials may not reflect all the information in the signal, since grand averaging can mask underlying effects [46],[124]. Recent improvements in computational power permit the real-time extraction of features from single-trial EEG recordings [66]. Single-trial EEG classification is currently widely used for decoding cognitive states and human intentions in neuroscience [16]. In a study based on visual perception tasks, ERP-derived features are also applied in object categorization [108]. Emotion-based BCIs typically exploit ERP components of brain signals that arise roughly 100 ms, 170 ms, and 230–270 ms after stimulus onset [14],[57],[68],[132]. In particular, the N170 and N200 ERP com-

ponents are known to discriminate between graded intensities of facial emotion [132]. Utilization of multiple ERP components provides complementary discriminatory power [108], and several studies now analyze ensembles of ERPs rather than individual ERP components [138]. Recent studies have indicated that several ERP components, including N100, P100, N170, N200, N300, and P300, are sensitive to the emotional stimuli [14],[57],[68],[144]. In one representative affective study, ERPs are computed by averaging electrodes over four scalp regions—left anterior (FP1, F3, F7, FC5, T7), right anterior (FP2, F4, F8, FC6, T8), left posterior (C3, CP5, P3, P7, O1), and right posterior (C4, CP6, P4, P8, O2)—to characterise affective processing [67]. Beyond emotion research, ERP and time-frequency analysis are also commonly applied to other fields including attentional mechanisms and task related factors [11],[32],[38],[125]. ERP measurement provides the ability to continuously evaluate human processing, enabling the identification of the various stages, such as attentional, cognitive, or perceptual stages, involved in performing an event [94]. Therefore, ERP components are utilized during the analysis of emotional and cognitive data in this thesis.

## 2.4 Wavelet Coherence

Wavelet analysis provides an inspection of the EEG signal in time and frequency domain by decomposing it into oscillatory component for different frequencies [13],[30]. Wavelet analysis brings effective analysis of the transient ERP signal that is non-stationary in nature [3],[2],[112]. The success of the wavelet features in the scaling and the shifting properties of the mother wavelet enables it to be applied in detecting brain diseases [2]. These wavelet-based approaches are especially important in seizure detection frameworks [41]. Wavelet analyses are commonly applied in emotional EEG research and gamma band activity is found to be discriminative for emotion classification in paradigms employing static emotional imagery as stimuli [78]. The delta, theta, and alpha bands might be complementary during resting-state emotion reading. Beta and gamma waves are appropriate for task-evoked emotion reading given its relevance with cognitive activities [77]. Therefore, a variety of frequency bands are investigated in this thesis. Time-frequency representations such as spectrogram,

Hilbert-Huang spectrum, and Zhao-Atlas-Marks transform are applied to discriminate the ratings of liking and consciousness [54]. Although many features, such as differential entropy [117], conventional statistical features [127], and wavelet-based indices [4], are obtained from individual channels, only a limited number are calculated across multiple channels to capture inter-channel dependencies [156], including the asymmetry of power spectral density between two hemispheres [155] and functional connectivity [146].

Wavelet coherence is commonly used to explore non-stationary signals via continuous wavelet transform. The relationship between two signals can be analyzed with wavelet coherence by estimating their spectral patterns and wavelet coherence is especially powerful tool for analyzing non-stationary signal [134]. Traditional spectral coherence measures the synchronization between two time series signals without temporal information, whereas wavelet coherence provides the coherence in the time-frequency space between two time series signals. In this way, the degree of connectivity between different signals and spatial patterns of these connections can be obtained among multiple EEG channels by applying wavelet coherence. Thus, the degree of connectivity among different EEG channels and the associated spatial patterns arising from these interactions can be determined. Consequently, this thesis investigates the applicability of wavelet coherence in the graph-theoretic approach.

The wavelet auto-spectrum of a signal $x(t)$ is given as in Eq. 2.1

$$W_{xx}(t,f) = \int_{t-\delta/2}^{t+\delta/2} S_x(\tau,f) \cdot S_x^*(\tau,f) d\tau \tag{2.1}$$

where $t$ and $f$ denote time and frequency and $^*$ is the complex conjugation.

$\delta$ is defined as the range of integration and is computed by $\delta = \frac{c}{f}$ where $c$ is the number of integration cycles in the wavelet window.

The wavelet cross-spectrum between two signals $x(t)$ and $y(t)$ is similarly defined as in Eq. 2.2

$$W_{xy}(t,f) = \int_{t-\delta/2}^{t+\delta/2} S_x(\tau,f) \cdot S_y^*(\tau,f) d\tau \tag{2.2}$$

Wavelet coherence is the normalized wavelet cross-spectrum and is given as in Eq. 2.3

$$WCoh_{xy}(t,f) = \frac{|W_{xy}(t,f)|}{\sqrt{W_{xx}(t,f).W_{yy}(t,f)}} \tag{2.3}$$

## 2.5 Graph-Based EEG Connectivity

The presence of connections among signals from different brain regions, which is a fundamental property of brain signals, is referred to as connectivity [20]. Connectivity in brain research denotes the dependence of brain function on the synchronous activity of neuronal assemblies spanning distinct cortical and sub-cortical regions. These functionally coupled neurons display temporally coherent activation patterns within a period of time. Electrophysiological data such as fMRI, EEG, and MEG data are commonly used to estimate interactions between different brain regions in connectivity-based studies [50]. Compared with other neuroimaging techniques, EEG offers high temporal resolution,frequency specification, and multiple source measuring. Consequently, functional connectivity enables the assessment of neural dynamics between specific brain regions [42]. Functional connectivity is employed to obtain features via multi-channels in several recent studies [79],[146]. Different methods are applied to infer functional relationships among distinct anatomical regions of the brain [40]. Nonlinear similarity measurement methods are well suited to analyze brain connectivity. Because mental functions and information processing result in established connections

between brain regions [9].

Traditional EEG signal analysis methods primarily investigate neural dynamics in the time and frequency domains, yet they do not consider consider spatial relationships among distinct brain regions. Graph theory is utilized to analyze functional connectivity patterns extracted from electrophysiological recordings in connectivity studies to inspect the organization of network patterns [122],[58]. It provides a robust and effective framework for multi-dimensional electrophysiological data analysis by considering both spatial and functional dependencies among brain regions [90]. Brain regions that are physically close tend to exhibit similar signal patterns due to the volume conduction effect, whereas activities of distant regions are mostly interrelated which can be characterized by some measures such as correlation, synchronization, coherence [133]. The connectivity information derived from these measures, in addition to mutual-information [148] and PLV values [49],[142], can be expressed in a graph-theoretic representation of the brain network [136]. By furnishing spatio-temporal information, wavelet coherence captures the dynamic and non-stationary features of neural signals, thus it delivers tangible enhancements over traditional correlation and mutual-information methods in functional connectivity analysis [25]. Moreover, window lengths are scaled inversely with frequency—employing shorter windows for high-frequency components and longer windows for low-frequency components. This is necessary for EEG signals as neural interactions frequently occur in short bursts [154]. Graph signal processing delivers a well-suited methodology for representing and analyzing signals with irregular structures by leveraging graph vertices [103]. Such an graph-based approach is appropriate for EEG signals, which are characterized by low spatial resolution, high dimensionality, and irregular structure [60]. Graph-theoretic metrics enable the characterization of EEG signals' stationary dynamics in cases where conventional linear methods alone lack sufficient explanatory power. When EEG signals are expressed in this manner, it becomes easier to provide opportunities to explore spatial relationships among different regions of the brain. Although there is a plenty of BCI-based emotion recognition studies, primarily utilizing single-channel-based feature extraction methods, in the existing literature, functional connectivity networks in the brain that are associated with emotion remain largely unexamined [147].

## 2.6 Graph Theory in Neuroscience

A graph can be defined as an abstract representation of a network consisting of vertices (nodes) and edges (connections), and edges denote the association among the vertices. An adjacency matrix $A$ gives information for the connectivity structure of the graph [40] and the element $W_{ij}$ encodes the weight of the directed edge from node $i$ to node $j$. If there is a weighted and directed edge exists from the node $i$ to $j$, then $W_{ij} \neq 0$, otherwise $W_{ij} = 0$, as shown in Figure 2.1.

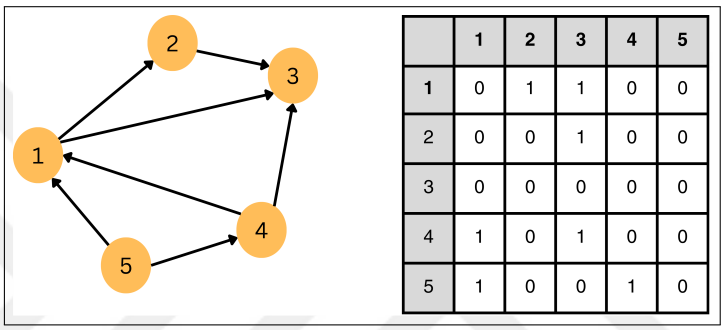


| | 1 | 2 | 3 | 4 | 5 |
|---|---|---|---|---|---|
| 1 | 0 | 1 | 1 | 0 | 0 |
| 2 | 0 | 0 | 1 | 0 | 0 |
| 3 | 0 | 0 | 0 | 0 | 0 |
| 4 | 1 | 0 | 1 | 0 | 0 |
| 5 | 1 | 0 | 0 | 1 | 0 |

**Figure 2.1** Adjacency matrix shown conceptually.

Graph edges can be categorized as weighted directed, unweighted directed, weighted undirected, and unweighted undirected. A directed edge allows information flows in one direction only, whereas an undirected edge allows flows in both directions along connected edges, as shown in Figure 2.2.

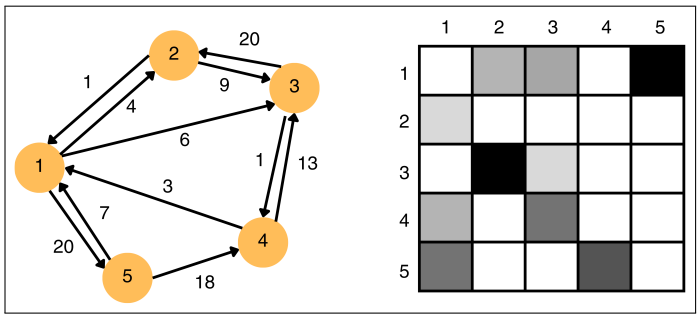


**Figure 2.2** Adjacency matrix shown in weighted matrix notation.

The weight assigned to an edge quantifies its connectivity strength, denoting strong and weak connections. In brain network graphs, links may represent anatomical, functional, or effective connectivity, so both weight and directionality must be specified.

Although binary directed networks indicate the existence or absence of connections, weighted directed networks indicate information about connection strengths.

The graph-theoretic based approach provides a powerful and promising framework for multi-dimensional neuroimaging analysis, as it accounts for both spatial and functional dependencies among brain regions [90]. Graph-theoretic analysis yields a suite of global and local metrics that quantify complementary aspects of network topology and performance. In this thesis, selected metrics from both categories are employed to discriminate (i) pleasant versus unpleasant emotional moods and (ii) low versus high cognitive load. This section explains several global and local graph metrics, such as energy, global efficiency, strength, transitivity, characteristic path length, and clustering coefficient, frequently cited in the literature [123] and used throughout this thesis.

*Energy :* Graph energy is defined as the sum of the absolute values of the eigenvalues of the graph's adjacency matrix [53]. Its formulation is as follows in Eq. 2.4.

$$Eng = \sum_{i=1}^{j} [\lambda_i] \tag{2.4}$$

where $\lambda_1$, $\lambda_2$,..., $\lambda_j$ are the eigenvalues of graph and $j$ is the graph order.

*Characteristic Path Length :* The characteristic path length is defined as the mean shortest path length across all pairs of nodes in the network [143]. Equivalently,it quantifies the efficiency with which information is transmitted across the network [40]. It is one of the global properties of the network structure and is the most commonly used metric of functional integration [111]. The equation used to calculate the weighted characteristic path length is given below in Eq. 2.5.

$$CPL = \frac{1}{A} \sum_{x \epsilon N} \frac{\sum_{y \epsilon N, y \neq x} d_{xy}^{W}}{A-1} \tag{2.5}$$

where $x$ and $y$ denote the nodes, $A$ is the number of vertices composing the graph and $d_{xy}$ denotes the shortest path between the nodes $x$ and $y$. The characteristic path length is primarily influenced by long paths in the network.

*Global Efficiency :* Efficiency coefficient of the path between two vertices is defined as the inverse of the shortest distance between the vertices. The average of all pairwise efficiencies is called the global efficiency [40], and its mathematical expression is given in Eq. 2.6 below:

$$Eff = \frac{1}{A(A-1)} \sum_{x \neq y \epsilon V} \frac{1}{d_{xy}} \tag{2.6}$$

where $A$ is the number of vertices composing the graph, $i$ and $j$ denote the nodes, and $d_{xy}$ denotes the shortest path between the nodes $i$ and $j$. Global efficiency measures how efficient the graph exchanges information at the global level. Global efficiency can be meaningfully calculated for disconnected networks, as paths in disconnected networks between nodes that are not connected are considered to have infinite length, resulting in zero efficiency. Global efficiency is mainly affected by short paths [111].

*Clustering Coefficient :* The tendency of nodes in a network to form highly connected clusters of vertices gives the clustering coefficient [40]. The clustering coefficient is obtained as the ratio of triangles (three fully connected nodes) to triplets (three nodes that are not fully connected) in the graph network [7]. That is, the clustering coefficient of $a$ node $b$ can be described as the fraction of the existing edges between the node in the neighborhood of node $b$ over the number of all possible edges among them. The clustering coefficient is calculated as in Eq. 2.7 [123].

$$CC_a = \frac{\sum_b \sum_c W_{ab} W_{bc} W_{ca}}{(\sum_b W_{ab})^2 - \sum_b {W_{ab}}^2} \tag{2.7}$$

where $a$, $b$, and $c$ denote the nodes and $W$ denotes the weight.

*Strength :* Sum of individual weights connecting to that node denotes the strength of a node $a$ ($Str_a$) and is calculated as in Eq. 2.8 [123].

$$Str_a = \sum_b W_{ab} \tag{2.8}$$

where $a$ and $b$ denote the nodes and $W_{ab}$ denotes the weight between the nodes a and b.

*Transitivity :* Transitivity is denoted as a variation of the clustering coefficient utilizing a different normalization method. It is generalized for weighted and directed graph networks [39, 102]. The transitivity of a network is calculated as in Eq. 2.9 [111].

$$Trs = \frac{\sum_{n \epsilon V} 2t_n}{\sum_{n \epsilon V} d_n(d_n - 1)} \tag{2.9}$$

where $V$ is the set of all nodes in the graph, $d_n$ is the degree of node $n$, $t_n$ is the number of triangles that include node $n$.

# 3. METHODOLOGY

In this thesis, emotional and cognitive EEG datasets as two distinct modalities are independently analyzed. The experimental paradigms and data acquisition methods for both dataset are detailed in this chapter.

## 3.1 Emotional Data Subjects

Thirteen healthy subjects with a mean age of 27.4 years (±2.96) were included in the study. EEG data were collected from 32 channels using a BrainAmp amplifier (Brain Products GmbH, Munich, Germany). Prior to the experiments, subjects were informed about the study, and signed informed consent was obtained.

The data were acquired in the Physiology Department of İstanbul Medical Faculty at İstanbul University. The data collection procedure received approval from the Local Ethical Committee of the Istanbul University Faculty of Medicine. The Local Ethics Committee of Istanbul University Faculty of Medicine approved the emotional data collection procedure (Approval Code: 2012/139-924; Approval Date: 30 January 2012).

## 3.2 Emotional Data Acquisition and Experimental Paradigm

Subjects were seated in front of a monitor (1920×1080 resolution 23 inch LED monitor) displaying the visual stimuli in a dimly lit recording room designed to minimize sound and electromagnetic interference. They were instructed to maintain focus on the center of the screen throughout the experiment. The stimuli were presented at a distance of one meter from the subjects, with each stimulus displayed on the screen for one second. The interval between stimuli was set to two seconds, as illustrated in Figure 3.1.

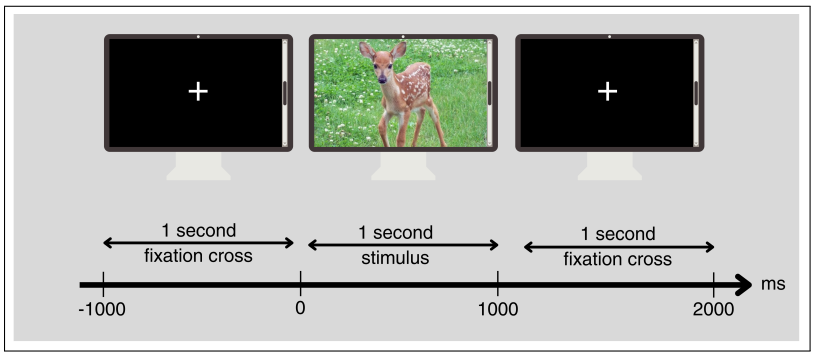


**Figure 3.1** Stimuli durations.

The experiment utilized a modified oddball paradigm to ensure subjects maintained attention to stimuli during the experiment throughout the passive condition. 280 pleasant and 280 unpleasant pictures with positive or negative emotional valence were presented as standard stimuli in two separate sessions, and a neutral stimulus was presented randomly as target stimulus. Emotional stimuli were selected as task-irrelevant to provide the isolated effect of emotion on ERP's. Pictures were selected from the IAPS dataset [74] with the mean valence level differing (7.13 / 2.96), but the mean arousal level being equal for the two sessions (4.99 / 5.02). Representative stimuli illustrating the pleasant and unpleasant image categories are presented in Figure 3.2.

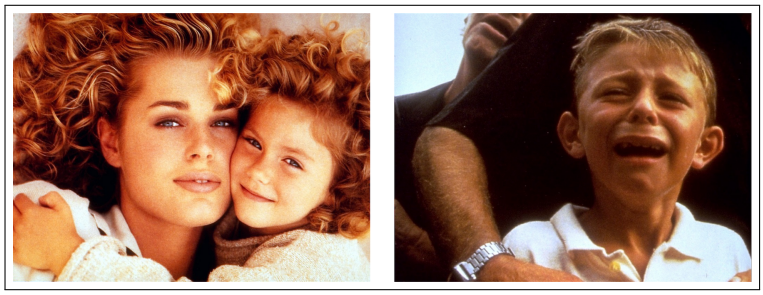

**Figure 3.2** Pleasant (left) and unpleasant (right) images [74].

To decrease order effect, half of the subjects' sessions were started with pleasant pictures while the other half of the subjects' sessions were started with unpleasant pictures. These two sessions can be seen in Figure 3.3.

The EEG data were recorded unipolar with reference to the mean of two ear lobes from 30 Ag/AgCl electrodes placed at FP1, FP2, F3, Fz, F4, FC3, FCz, FC4,

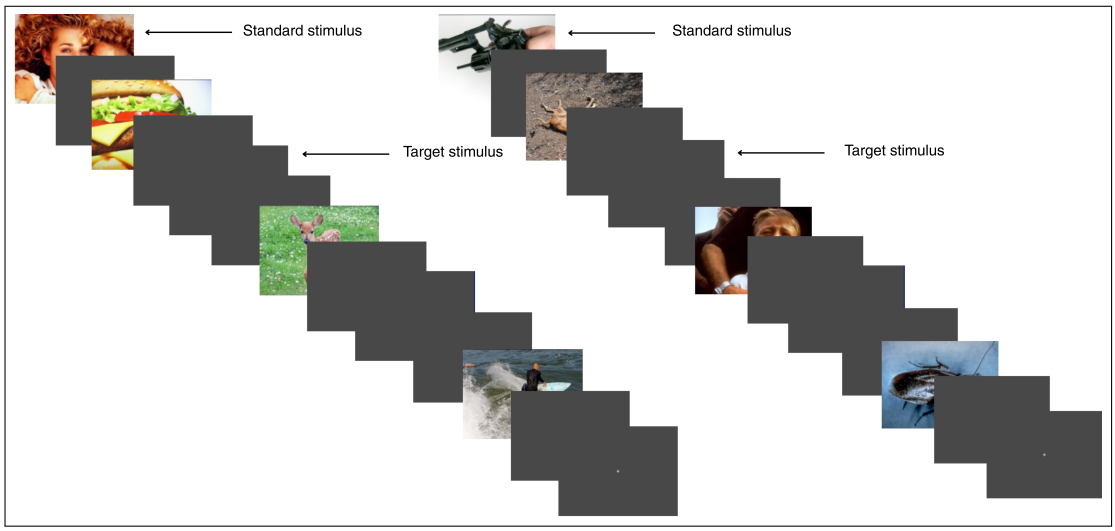


**Figure 3.3** Emotional stimuli.

F7, F8, FT7, FT8, C3, Cz, C4, CP3, CPz, CP4, T7, T8, P3, Pz, P4, TP7, TP8, P7, P8, O1, Oz, O2 according to the international 10–20 system, referenced to electrodes on both ear lobes. EOG was measured using electrodes positioned on the nasal and outer canthus of the right eye to track eye movements.

## 3.3 Cognitive Data Subjects

Cognitive data were obtained from 15 healthy subjects aged from 22 to 35, none of whom had acute or chronic neurological or psychiatric disorders or were pregnant women. Among them, eleven of them were right-handed, and ten were male.

The data were recorded using a BrainAmp amplifier and 64 active electrodes (Brain Products GmbH, Munich, Germany) arranged according to the 10–20 international system. An EOG electrode was positioned below the left eye to record eye movements [98]. Unipolar recording was performed at a sampling frequency of 1 kHz., with the ground electrode placed at position $AF_z$ on the scalp and the reference at the left mastoid. The acquisition system was later re-referenced to the left and right mastoids. Electrode impedance was maintained below 20 kΩ during cap placement.

All data were collected at Technische Universität Berlin after obtaining formal approval from the university's Ethical Review Board [98, 100]. Cognitive data were obtained from the DepositOnce repository of Technische Universität Berlin (https://depositonce.tu-berlin.de/handle/11303/6747, accessed on 17 April 2020).

## 3.4 Cognitive Data Acquisition and Experimental Paradigm

The stimuli were designed using vector graphics created with Inkscape software [98] and images from the animals category, provided by Freepik and sourced from the Freepik database [98]. Stimuli presentation was displayed on a 24 inch LED monitor with a 60 Hz. refresh rate and a resolution of 1920×1200 resolution. The experimental paradigm was developed using Processing software [98] in combination with MATLAB software (release R2014a, The MathWorks, Inc., Natick, MA, USA) for signal acquisition. Fifteen subjects viewed a sequence of visual stimuli featuring cartoon representations of fruits, animals, and transportation devices, performing specific tasks associated with each stimulus type, as illustrated in Figure 3.4.

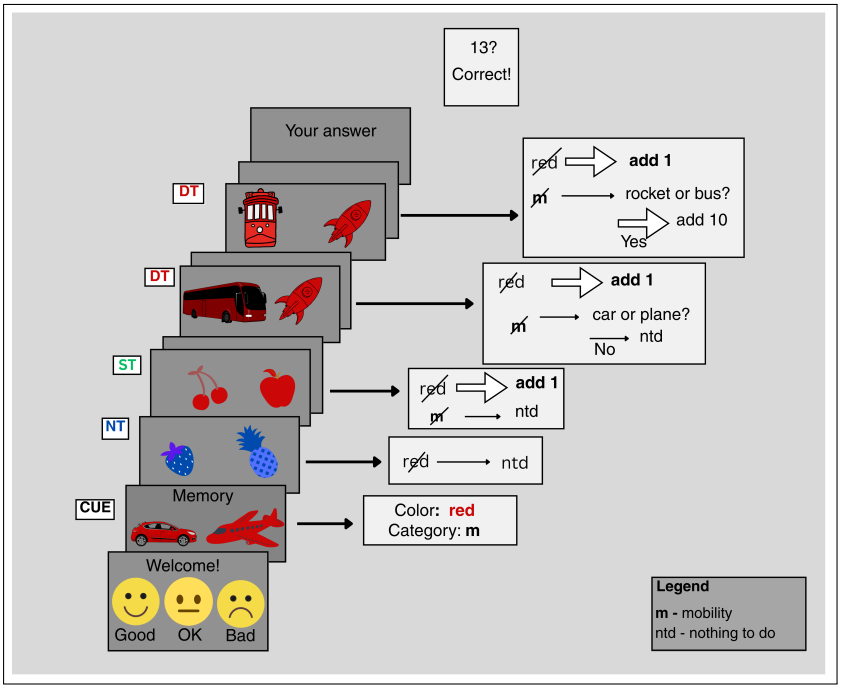


**Figure 3.4** Cognitive paradigm [98].

Three levels of cognitive processing were investigated: no processing, shallow processing (requiring stimuli differentiation based on color), and deep processing (imposing the performing of a complex activity related to cognitive process). Each visual stimulus consisted of a pair of two cartoon images, which represented an object among three categories: animals, fruits, and mobility, and they were represented in one of the red, green, blue, or magenta colors. Both images had the same color and the same category, where each category consisted of a total of 10 objects [98]. Only two of the three categories were chosen for each run to keep the desired ratio and without increasing the difficulty of the tasks too much. Subjects were required to remain seated, relaxed, and focused during the experiments conducted in a laboratory setting. They were allowed to freely explore the presented information but were primarily instructed to focus their gaze on the center of the screen. Each subject completed a practice test (1–3 runs) to familiarize themselves with the tasks.

In the experimental paradigm, after a brief self-assessment of their current state, subjects were shown the condition to be performed along with a target image pair, defined by color and category. When the sequence began, they first had to discriminate based on color and then on category. No processing was required (Non-Target, NT case) if the color did not match the target. If only the color matched, the subjects performed a mental computation (Shallow Target, ST case). However, when both the color and the category matched the target (Deep Target, DT case), a related cognitive task and corresponding mental computations were required for evaluation.

Following by the feedback regarding the correct number, the result was recorded at the end of each run. Each cognitive task, which are memory, language, and visual imagination, respectively, was conducted with five runs per condition. To prevent confusion between tasks, the conditions were not alternated after each run. Among three different cognitive tasks, the memory task, considering memory retrieval by comparing a previously presented stimulus with the current stimulus, has been selected as related to the cognitive workload for analysis in this thesis. Memory retrieval in this task involves comparing a previously presented stimulus with the current stimulus [67]. The task involved determining whether the current stimulus matched the previous tar-

get pair (specifically, the last target color and category). Accomplishment required memorizing the current pair and retrieving the previous target pair for comparison.

A total of 600 trials, consisting of five runs, each lasting 1.25 seconds, were presented divided in 75% for NP and 12.5% for SP or DP cases to maintain the occurrence proposed for positive targets [99]. A total of 120 stimuli, each consisting of a pair of two images with the same color (red/green/blue/magenta) were presented after presentation of a cue. Each image pair depicted different objects selected from the categories of animals, fruits, and mobility, with each category containing a total of ten objects. Experiment timing is shown in Figure 3.5. Inter-stimuli interval is 2500 ms., comprising 500 ms. of fixation, 1250 ms. of stimulus presentation and a 750 ms. relaxation period.

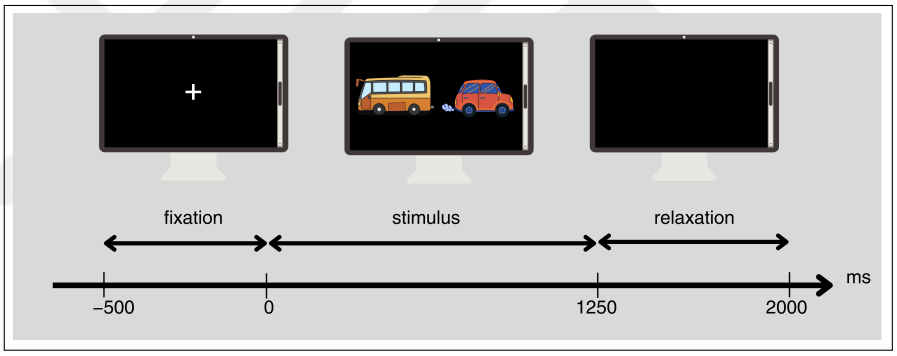


**Figure 3.5** Memory stimuli experiment timing.

# 4. EMOTIONAL DATA ANALYSIS AND RESULTS

This chapter presents a structured analysis of emotional data using graph-theoretic metrics and wavelet coherence-based classification applied to single-trial ERP components. The rest of the chapter outlines the analytical workflow for the emotional dataset, covering preprocessing, time–frequency decomposition, and graph-theoretical analysis.

## 4.1 Preprocessing

EEG data were collected with a sample rate of 250 Hz. and then band-pass filtered between 0.1 Hz. and 40 Hz. with a zero-phase, sixth-order Butterworth filter to isolate the frequency components of interest. Subsequently, 50 Hz. notch filter was applied to suppress line noise. Artifact rejection proceeded via a two-stage protocol. First, a max–min routine excluded epochs whose absolute amplitude exceeded 100 µV or whose peak-to-peak difference surpassed 150 µV in any channel. Second, artifacts caused by eye blinks or facial movements detected in bipolar EOG recordings were isolated and removed from the EEG by independent component analysis (ICA) implemented in EEGLAB [29], following visual confirmation of the contaminating components.

Raw EEG data were first inspected with a detailed visual inspection to catch abnormal patterns caused by artifacts, spikes, sustained flat-lines, and broadband noise. Residual high-frequency contamination, including 50 Hz. line interference, was then attenuated via spectral filtering. Another criterion for artifact identification was the abnormality in the duration or amplitude of a signal. Any signal exceeding a definite value not compatible with a typical EEG pattern was noted as an artifact. All artifact decisions were confirmed by experienced clinical neuropsychologists, thereby ensuring the validity of the cleaned dataset.

Independent component analysis (ICA) was conducted with the Infomax algorithm in EEGLAB. This linear decomposition method permits for the identification of irrelevant or undesired constituents of the signal, which can be easily identified as artifacts by visual inspection. Following artifact removal, EEG data were decomposed into epochs. The epochs were segmented into 1200 ms windows extending from −200 ms to +1000 ms relative to stimulus onset (0 ms). Baseline correction was applied for the 200 ms preceding the presentation of the stimulus.

## 4.2 ERP Analysis

After removal of the artifacts, the remaining valid responses for each stimulus type were averaged for each subject. The grand average for each electrode was computed by averaging across subjects to obtain ERPs associated with pleasant and unpleasant stimuli. The ERPs measured against each stimulus were obtained by taking the average of epochs which are time-locked to a defined event and this is one of the commonly used methods in EEG data analysis [85]. Therefore, epochs corresponding to the pleasant and unpleasant data were separately averaged across all subjects to see if there was a differentiation between the ERP results of subjects during the presentation of pictures having pleasant and unpleasant emotional effects.

The grand average ERP waveforms in the F3, F4, Fz, and Cz channels evoked by the pleasant and unpleasant stimuli are shown in Figure 4.1, Figure 4.2, Figure 4.3, and Figure 4.4, respectively. Upon analyzing the ERP differences between the pleasant and unpleasant stimuli over all channels, it was clearly seen that there are deflections in ERP amplitude during specific post-stimulus latency windows at several channels between two emotional moods.

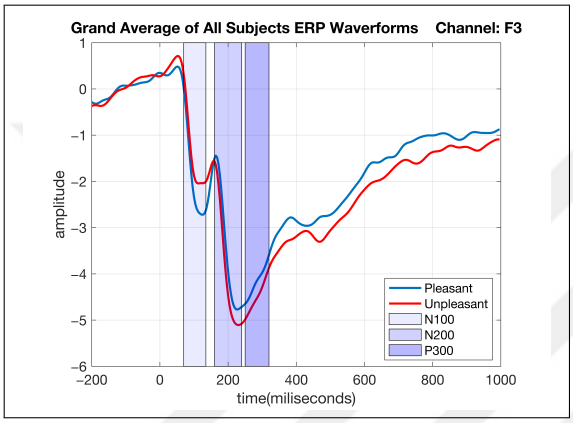


**Figure 4.1** ERP waveform of F3 channel.

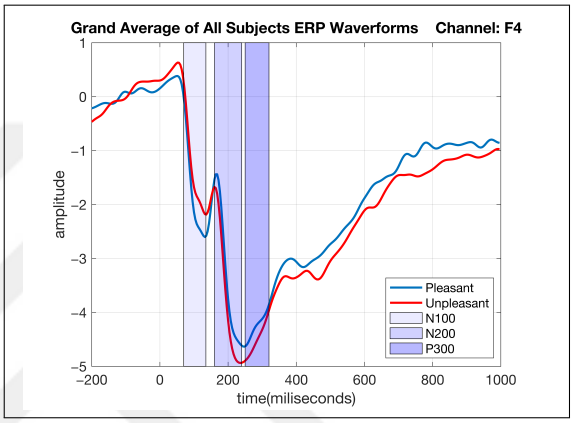


**Figure 4.2** ERP waveform of F4 channel.

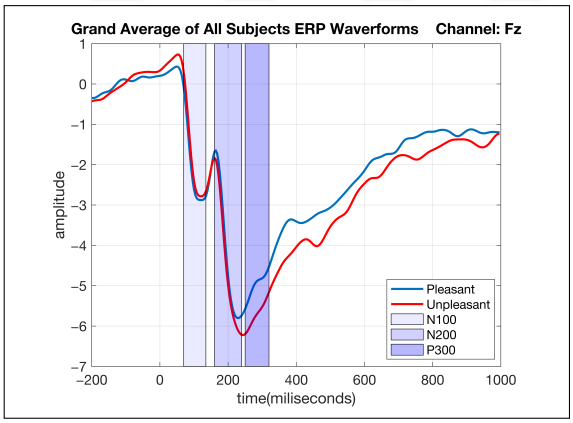


**Figure 4.3** ERP waveform of Fz channel.

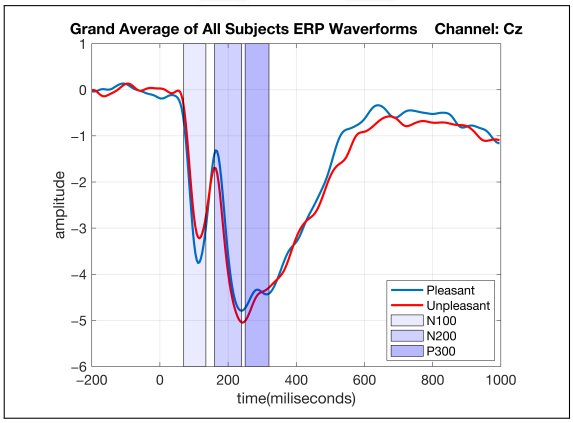


**Figure 4.4** ERP waveform of Cz channel.

## 4.3 Wavelet Analysis

Although Fourier analysis reveals only the frequency content, it does not provide any information about the temporal localization of those frequencies. Wavelet analysis, in contrast, provides information about both frequency and time within signals. Use of the wavelet transform to generate features of electroencephalography (EEG) signals has provided researchers a new tool to investigate the time-frequency characteristics of the signal, as brain activity is highly time-dependent. Among wavelet-based approaches, the discrete wavelet transform (DWT) has been extensively used in more scientific work than continuous wavelet transform (CWT) [41]. Efficiency in suppressing redundancy, easy implementation, and lower computation time make DWT more preferable than CWT [72]. DWT can efficiently decompose non-stationary signals into sub-frequency bands. In this thesis, the biorthogonal3.7 (*bior*3.7) wavelet, widely adopted in biomedical applications [137],[45],[24], was selected to decompose each epoch into delta (0–4 Hz.), theta (4–8 Hz.), alpha (8–16 Hz.) and beta (16–32 Hz.) frequency bands for every trial across all subjects.

The wavelet coefficients of the delta, theta, alpha, and beta frequency bands for each ERP epoch were calculated for each subject and each trial to investigate the differentiation between pleasant and unpleasant stimuli effects. Four discrete wavelet functions, namely daubechies (*db*1 and *db*4 ), bioorthogonal (*bior*3.7) and symlet(*sym*8), were selected in the computation. Band-specific coefficients were subsequently grand-averaged across all subjects, enabling a comparison of these wavelet functions, to decide which provided the most discriminative representation for classifying pleasant and unpleasant EEG signals. After obtaining the best performance with the *bior*3.7 wavelet function, the *bior*3.7 wavelet function was employed to compute coefficients for the delta, theta, alpha, and beta frequency bands in ERP segments across all trials and subjects. The mean of the wavelet coefficients in four bands corresponding to the N100, N200, and P300 ERP components were selected as features during the classification. k-NN, LDA and SVM methods were used to discriminate pleasant and unpleasant emotional moods. The same procedure was subsequently repeated by selecting the energy of wavelet coefficients as feature set.

The three different ERP components, the N100, associated with sensory activation; the N200, originating primarily from the anterior cingulate and fronto-central regions; and the P300, reflecting parietal-frontal connectivity, were hypothesized to represent stages within a hierarchical model that elucidates the neural mechanisms underlying emotion and cognition on a millisecond scale [70]. Consequently, these ERP intervals were utilized in wavelet analysis to accurately discriminate emotional moods and cognitive states.

After obtaining wavelet coefficients for the N100, N200, and P300 ERP components, seven hierarchical feature configurations were assembled: the individual components (N100, N200, P300), their pairwise concatenations (N100–N200, N100–P300, N200–P300), and the composite window spanning entire components (N100–N200–P300). For each hierarchical configuration and for every frequency band, two complementary descriptors, namely the band-specific mean of the wavelet coefficients and the band-specific energy of wavelet coefficients computed. Consequently, 14 distinct feature sets were formed for each EEG frequency band. Feature extraction encompassed 30 channels, namely Fp1, Fp2, F7, F3, Fz, F4, F8, FT7, FC3, FCz, FC4, FT8, T7, C3, Cz, C4, T8, TP7, CP3, CPz, CP4, TP8, P7, P3, Pz, P4, P8, O1, Oz and O2.

For each subject separately, classification accuracy, sensitivity, and specificity were computed and then averaged across all subjects to obtain grand average performance metrics, hence assessing the impact of feature set selection on classification efficacy. k-NN, LDA and SVM classification methods were used in discrimination stage. Figure 4.5 shows the grand average accuracy, sensitivity, and specificity achieved by k-NN for the various sets of delta band features. The mean and energy of the wavelet coefficients were extracted from seven ERP components: the individual N100, N200, and P300 components; the concatenated pairs N100–N200, N100–P300, and N200–P300; and the entire N100–N200–P300 component. According to the grand average classification results, the highest classification accuracy, 56.3%, in delta band was achieved when the feature set was limited to the mean of the wavelet coefficients associated with the N100–N200 ERP components.

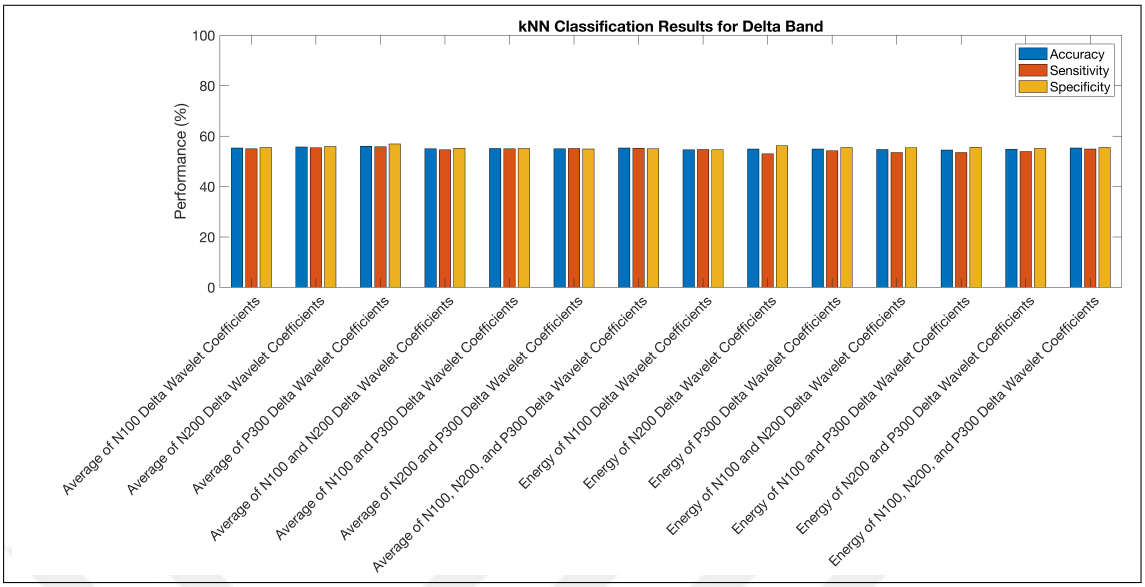


**Figure 4.5** k-NN classification results.

Using identical feature configurations, Figure 4.6 shows the grand-average accuracy, sensitivity, and specificity attained in the delta band when classification was performed with the LDA algorithm. Within the delta band, the LDA classifier achieved its peak grand-average accuracy of 67.5% when the feature set was restricted to the mean of wavelet coefficients corresponding to the N200–P300 ERP components.

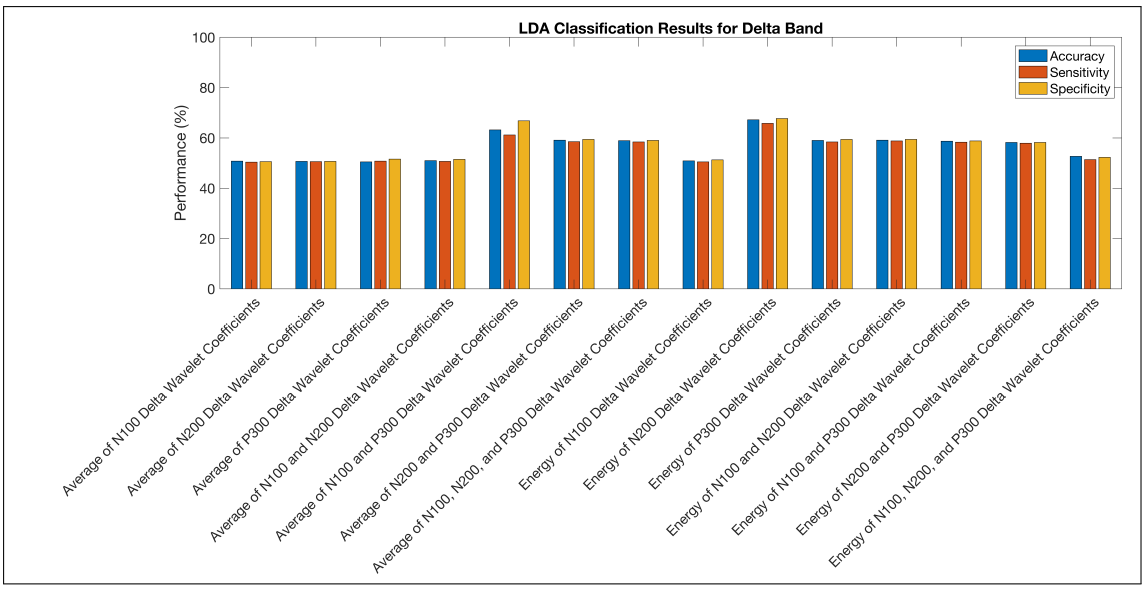


**Figure 4.6** LDA classification results.

Finally, the SVM classifier was applied to the beta band with the same feature configurations assessed in the previous analysis; the resulting grand-average accuracy, sensitivity, and specificity rates were presented in Figure 4.7. The SVM classifier achieved its highest grand-average accuracy of 61.2% in the delta band when the feature vector was restricted to the energy of the wavelet coefficients associated with the N100–N200 ERP components.

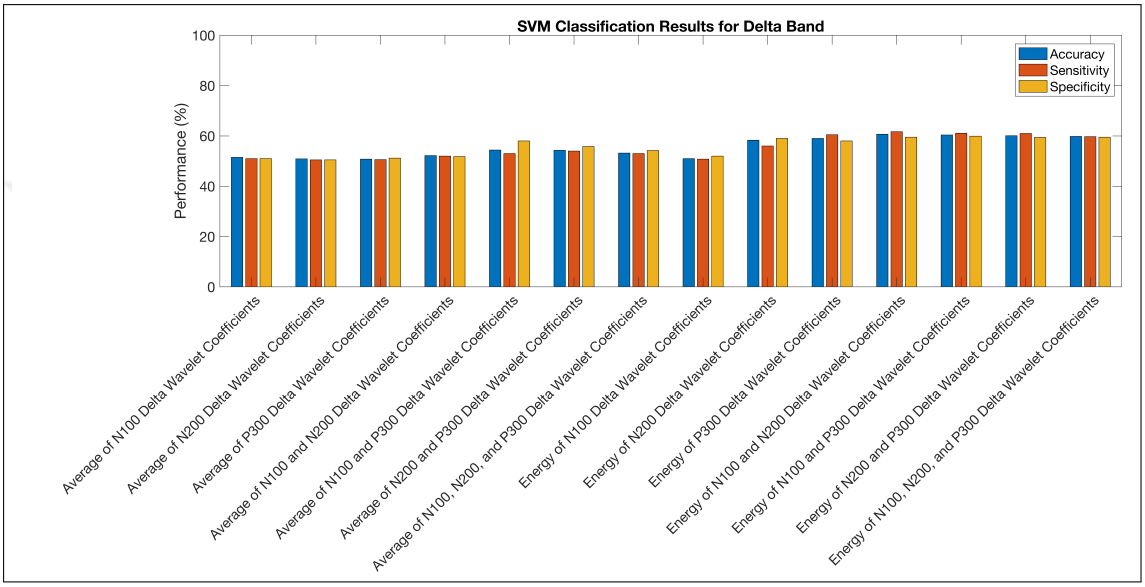


**Figure 4.7** SVM classification results.

Subsequently, the theta band was analyzed with k-NN, LDA, and SVM classifiers, using the same feature configurations and ERP components employed for the delta band. Figure 4.8 presents the grand-average accuracy, sensitivity, and specificity yielded by the k-NN classifier across the various set of theta band features. Both the mean and energy of the wavelet coefficients extracted from the predefined ERP components were evaluated as features. The highest grand-average accuracy of 57.9% was attained by selecting energy of wavelet coefficients as feature set in the theta band corresponding to the P300 ERP component.

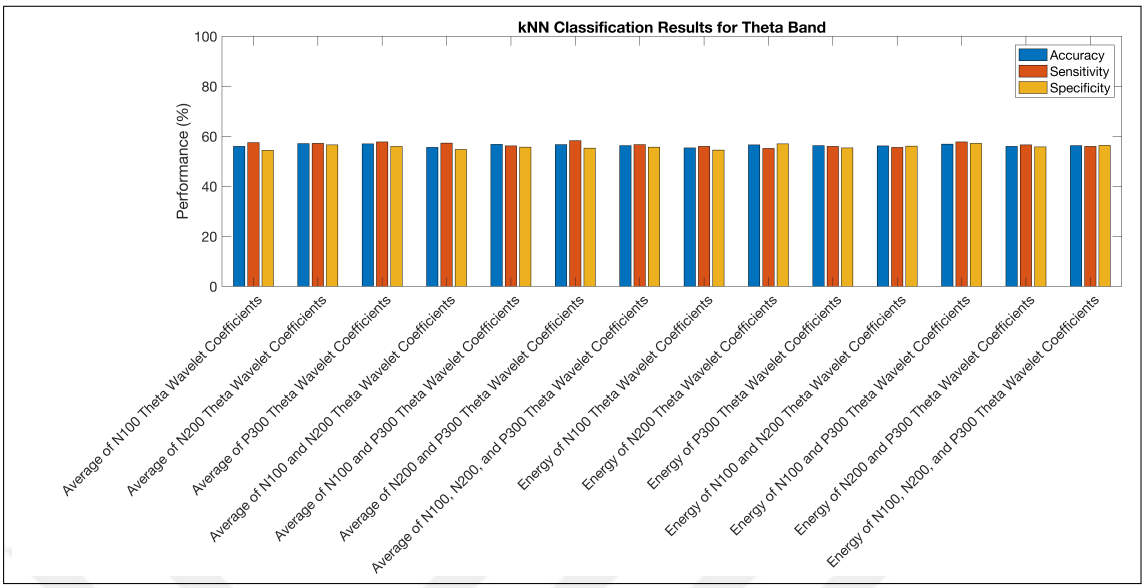


**Figure 4.8** k-NN classification results.

In the theta band analysis with LDA, both the mean and energy of the wavelet coefficients from each ERP component were tested as feature sets. The highest grand-average accuracy of 64.7% was achieved when the feature set was restricted to the wavelet energy coefficients associated with the P300 ERP component, as shown in Figure 4.9.

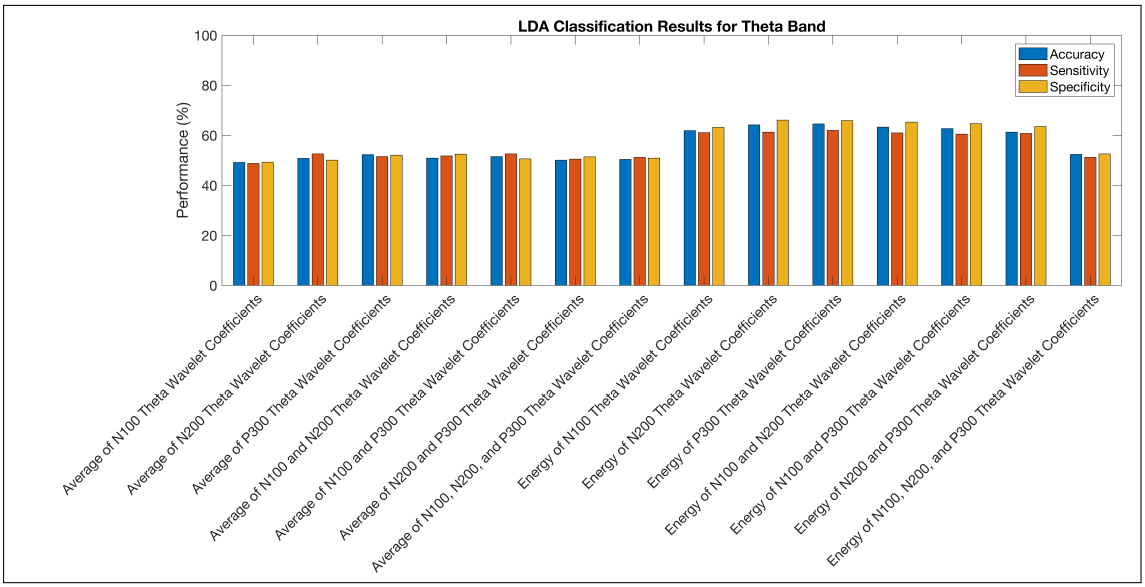


**Figure 4.9** LDA classification results.

When the feature vector likewise comprised solely of the wavelet energy coefficients corresponding to the P300 component, feature sets yielded a peak grand-average accuracy of 66.0% by applying SVM to the theta band, as shown in Figure 4.10.

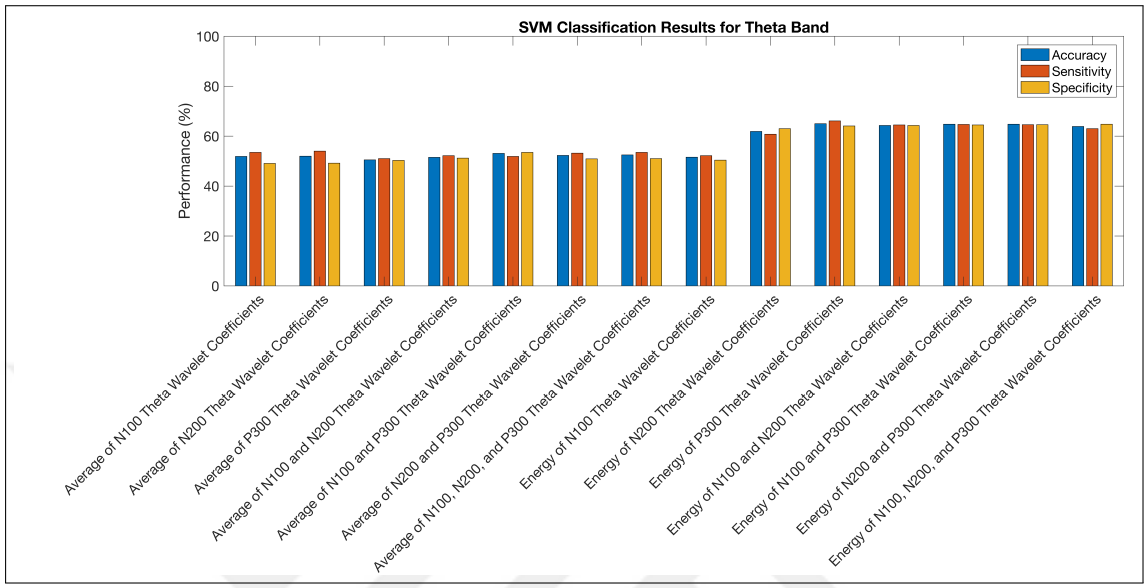


**Figure 4.10** SVM classification results.

The same procedure was replicated for the alpha band. Using k-NN, the highest grand-average accuracy of 60.1% was obtained when the feature set consisted of the mean wavelet coefficients associated with the N100–N200 components, as shown in Figure 4.11.

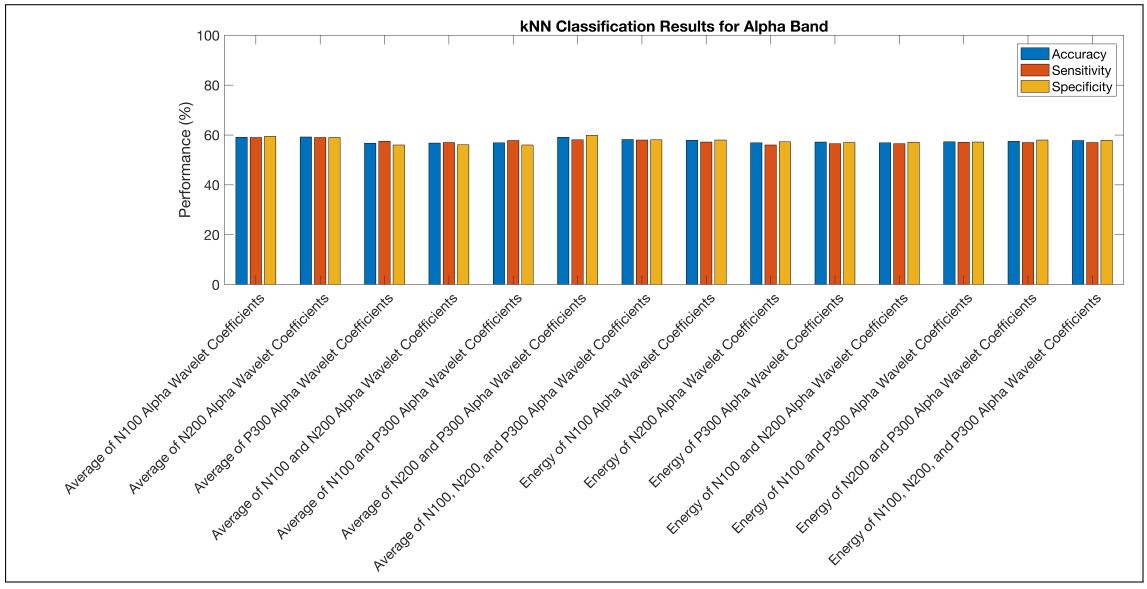


**Figure 4.11** k-NN classification results.

Subsequently, LDA was applied to the alpha band data with feature sets consisting of both the mean and energy of the wavelet coefficients corresponding to various ERP components. The slassification performances were demonstrated in Figure 4.12. The highest grand-average classification accuracy of 67.4% in the alpha band was attained when the feature vector comprised the energy coefficients corresponding to the N100–P300 components.

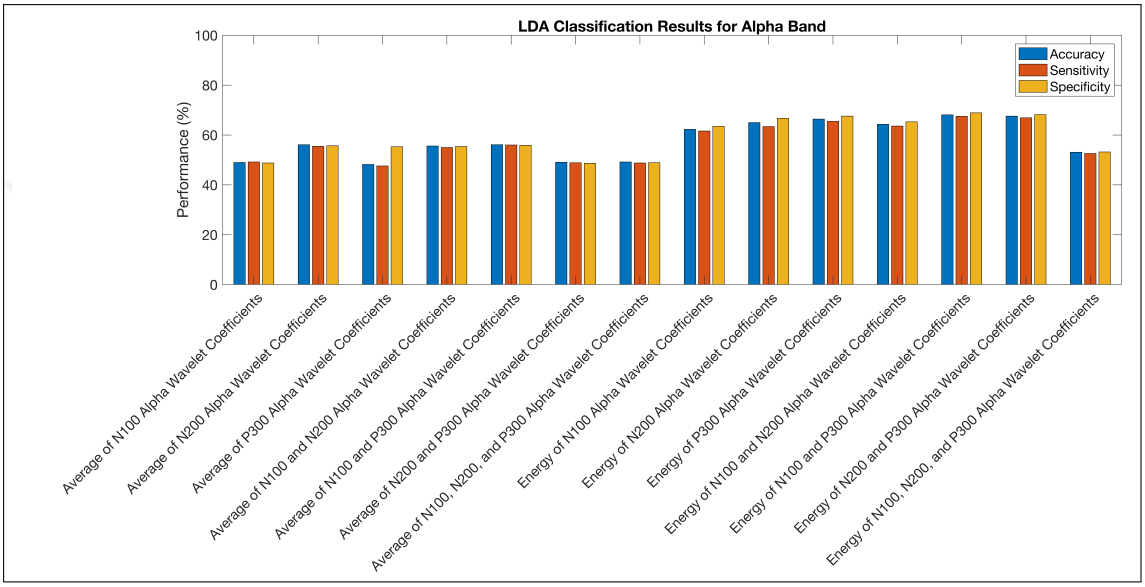


**Figure 4.12** LDA classification results.

Later, the SVM classifier, evaluated with the same feature configurations, reached an improved peak accuracy of 69.1% when the feature set was limited to the energy coefficients of the P300 component, as depicted in Figure 4.13.

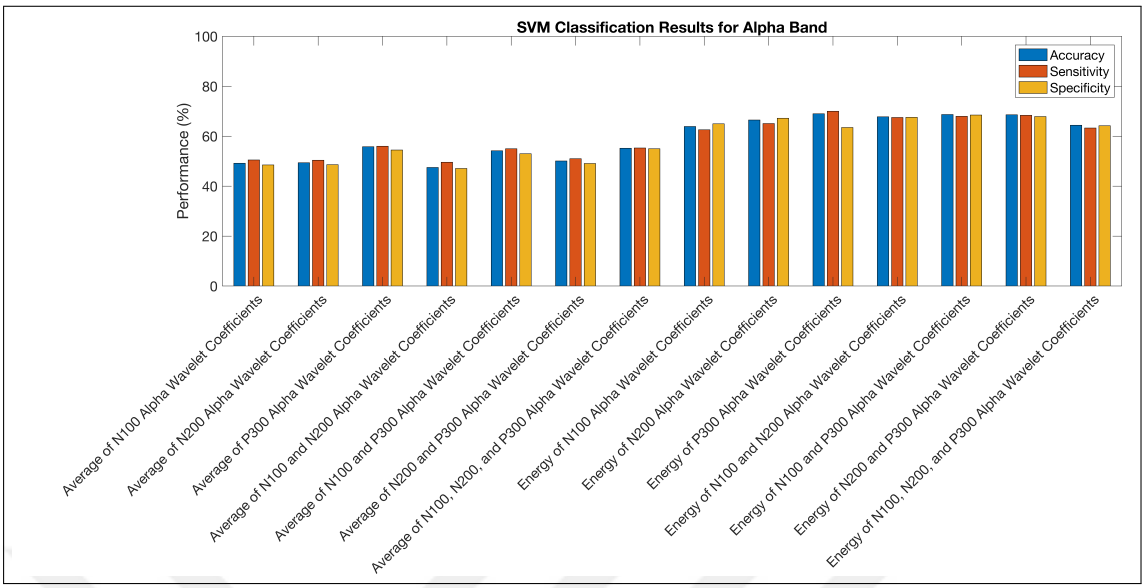


**Figure 4.13** SVM classification results.

Thereafter, discrimination in the beta band was measured as in previous analyses. Feature vectors were constructed from the mean and energy of the wavelet coefficients extracted from several combinations of ERP components. For the k-NN classifier, Figure 4.14 summarizes the grand-average accuracy, sensitivity, and specificity. The highest classification accuracy of 69.2% was obtained when the feature set comprised wavelet coefficients spanning the N200–P300 ERP components.

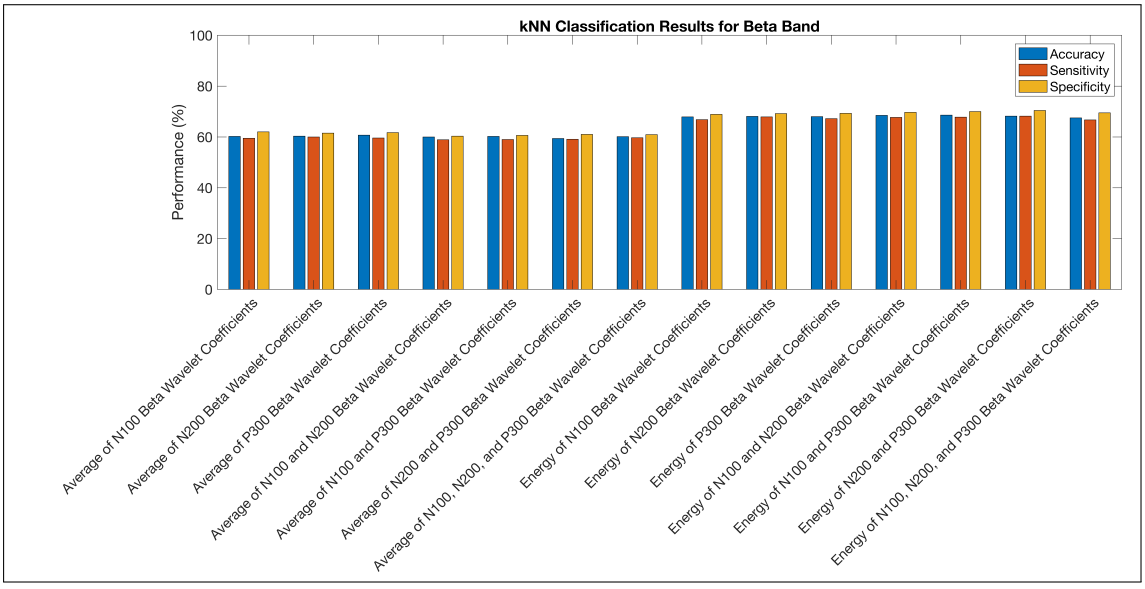


**Figure 4.14** k-NN classification results.

Figure 4.15 presents the results of the LDA classifier in the beta band obtained with the same feature configurations, reporting grand-average accuracy, sensitivity, and specificity. The highest accuracy of 78.5% was obtained when the feature vector comprised the energy coefficients of the N200–P300 components.

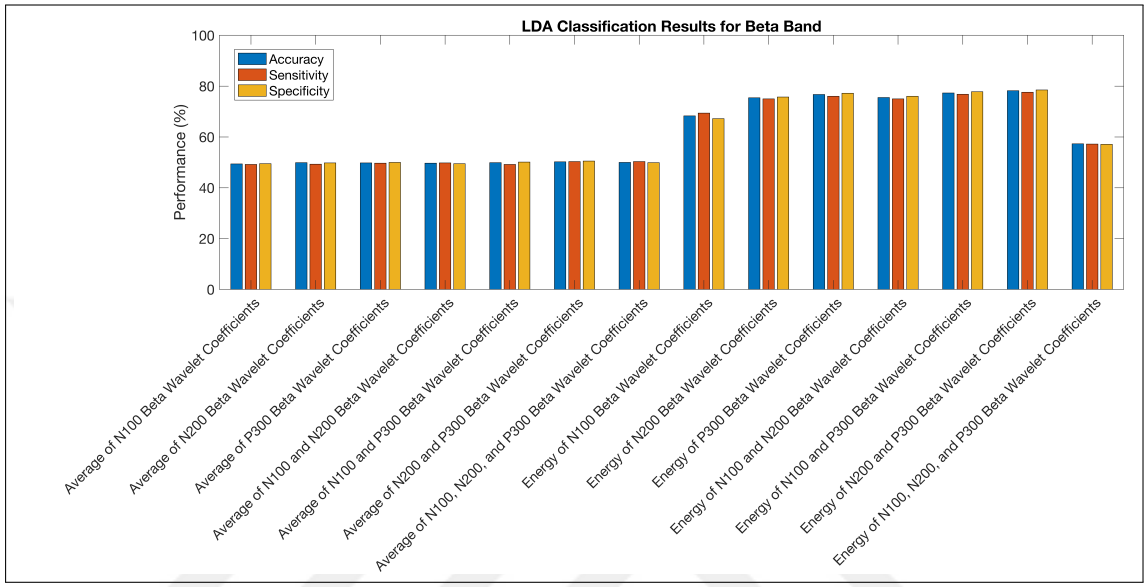


**Figure 4.15** LDA classification results.

Lastly, identical feature sets were then assessed with the SVM classifier; as shown in Figure 4.16, SVM likewise achieved its optimal performance when using the energy coefficients corresponding to the N200–P300 components.

Classifying each subject individually, the grand-average metrics attained were 81.1% for accuracy, 81.9% for sensitivity, and 81.5% for specificity. Across all combination of feature of ERP components, SVM classification in the beta band yielded the best overall performance, with its peak results consistently emerging when the feature vector included the energy of the wavelet coefficients from the N200–P300 components. Accordingly, this most discriminative feature set was adopted for the final per-subject analysis. The resulting classification accuracy, sensitivity, and specificity rates obtained for each subject individually were presented in Table 4.1.

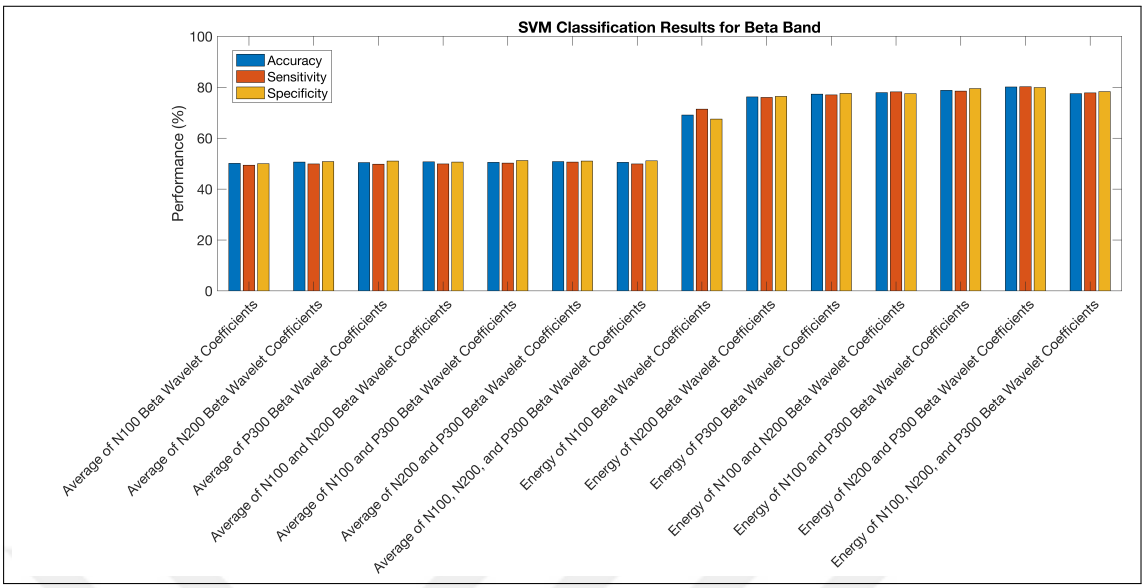


**Figure 4.16** SVM classification results.

**Table 4.1**
Classification performance for each subject by using energy of N200 and P300 beta wavelet coefficients.

| | Accuracy | Sensitivity | Specificity |
|---|---|---|---|
| Subject-1 | 91.8 | 93.4 | 90.3 |
| Subject-2 | 71.1 | 64.8 | 77.4 |
| Subject-3 | 77.0 | 78.3 | 75.6 |
| Subject-4 | 95.1 | 93.4 | 96.6 |
| Subject-5 | 81.7 | 88.4 | 75.4 |
| Subject-6 | 85.6 | 85.9 | 85.4 |
| Subject-7 | 84.4 | 88.1 | 80.6 |
| Subject-8 | 68.2 | 68.4 | 68.0 |
| Subject-9 | 86.2 | 85.0 | 87.4 |
| Subject-10 | 73.6 | 70.2 | 77.1 |
| Subject-11 | 75.2 | 77.8 | 72.5 |
| Subject-12 | 82.8 | 79.6 | 86.0 |
| Subject-13 | 81.0 | 78.3 | 90.2 |

The best performance was achieved with the SVM classifier when the feature vector comprised the beta band wavelet energy coefficients of the N200–P300 interval.

Given the accuracy, sensitivity, and specificity values per each subject summarized in Table 4.1, the top-performing subject reached an accuracy of 95.1% under individual-subject modeling.

## 4.4 Wavelet Coherence

Initial classification attempts based on wavelet coefficients yielded only modest performance, indicating limitations in their ability to extract the discriminative features of the EEG signals. Given these suboptimal results, alternative approaches were explored to improve the classification accuracy. Consequently, wavelet coherence was employed, as it provides a more robust representation by capturing both time–frequency information and functional connectivity patterns between EEG channels.

Wavelet coherence was computed using MATLAB R2024a with the Signal Processing Toolbox, following the algorithm of [52]. Morlet wavelet was used as the prototype function in wavelet analysis. The minimum and maximum scales were chosen so that lowest frequency was restricted by the signal length and the wavelet's time-frequency extent and highest frequency was limited by the Nyquist frequency. The number of scales was $\text{floor}(\log_2(N)) - 1$, where $N$ was the number of samples in input signal.

Wavelet coherence values corresponding to the N100, N200, and P300 time intervals were calculated across all channels separately for each trial and each subject within the basic EEG frequency bands, namely delta, theta, alpha, and beta. This was realized for both data corresponding to the pleasant and unpleasant paradigms.

Before investigating each subject individually, the averages of all of the subjects' wavelet coherence values over all the trials were obtained for N100 ERP component, and the connectivity map, denoting the difference in wavelet coherence values between pleasant and unpleasant conditions, was obtained as seen in Figure 4.17.

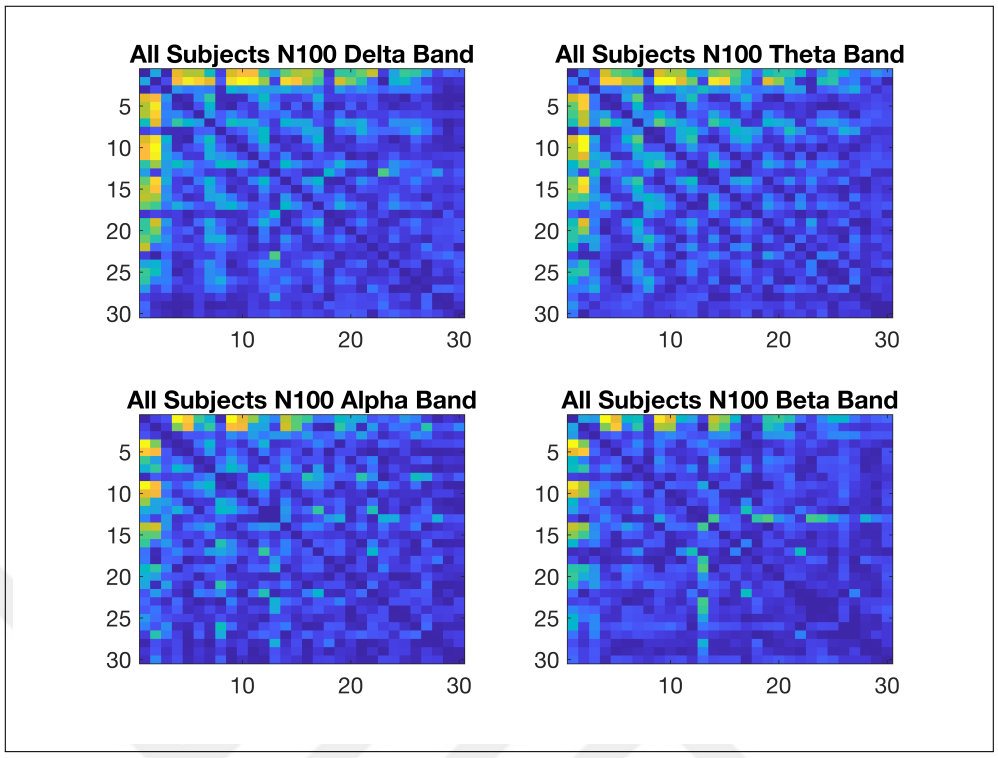


**Figure 4.17** N100 connectivity maps of difference for delta, theta, alpha, and beta frequency bands.

Connectivity maps corresponding to the wavelet coherence difference for pleasant & unpleasant emotional moods were also obtained across all channels and frequency bands for the N200 and P300 ERP components. Wavelet coherence difference maps associated with the N200 and P300 ERP components were also plotted, as shown in Figure 4.18 and Figure 4.19, respectively. EEG channels, namely FP1, FP2, F3, Fz, F4, FC3, FCz, FC4, F7, F8, FT7, FT8, C3, Cz, C4, CP3, CPz, CP4, T7, T8, P3, Pz, P4, TP7, TP8, P7, P8, O1, Oz, and O2 were numbered from 1 to 30 on both axes. Lighter hues indicate larger differences, whereas darker hues denote smaller ones in the figures.

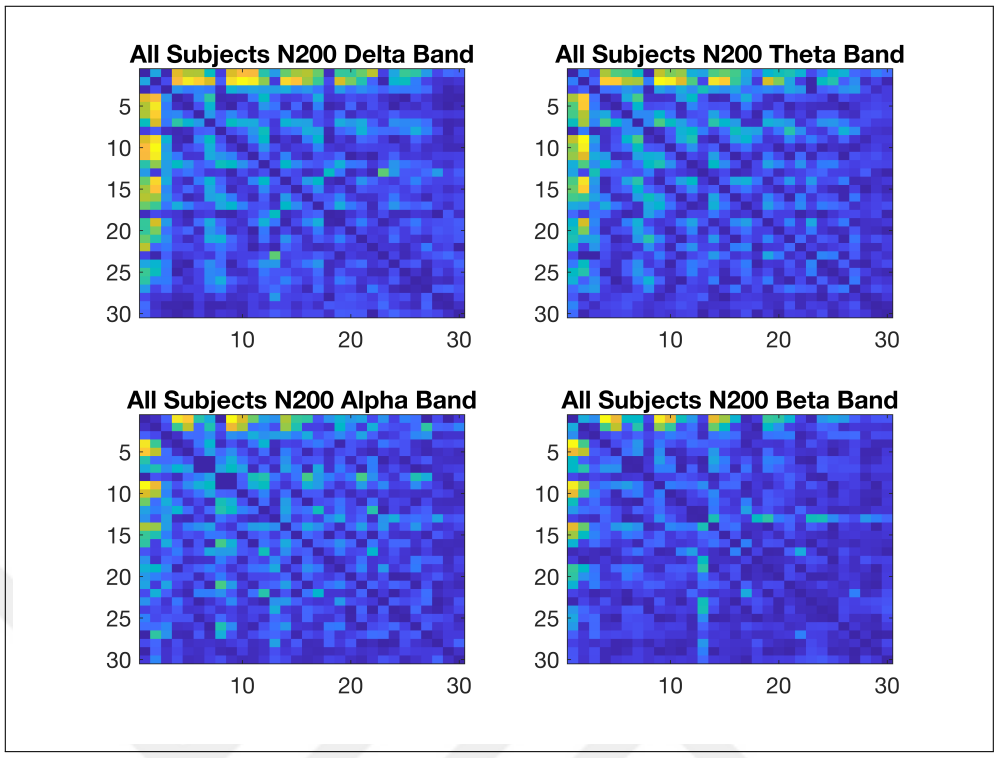


**Figure 4.18** N200 connectivity maps of difference for delta, theta, alpha, and beta frequency bands.

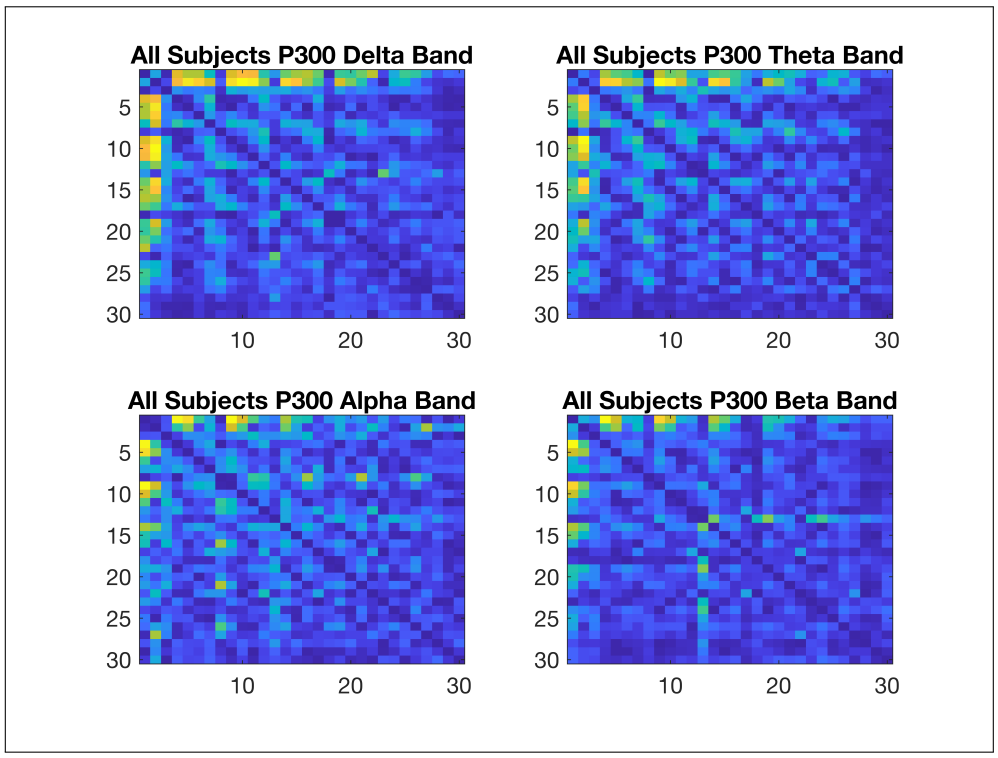


**Figure 4.19** P300 connectivity maps of difference for delta, theta, alpha, and beta frequency bands.

## 4.5 Graph-Theoretic Metrics

Global and local graph metrics can be applied to extract the global and local properties of the network, thereby characterizing the network's topology. In this thesis, several global and local graph metrics were utilized to discriminate pleasant and unpleasant emotional moods as well as low and high cognitive states. In the context of emotional and cognitive EEG data analysis using graph-theoretic metrics, the wavelet coherence matrix was employed to construct the adjacency matrix.

Graph-theoretic metrics based techniques were applied by interpreting wavelet coherence information within a graph-structured framework because the adjacency matrix was consisted of wavelet coherence values calculated among EEG channels. To do this, wavelet coherence values served as edge weights representing connectivity between nodes (channels) of the graph. The combination of graph-theoretic metrics and wavelet coherence is particularly advantageous due to their combined capability to analyze signals defined on complex, non-Euclidean domains. By applying wavelet coherence analysis to signals structured as graphs, it became possible to comprehensively evaluate both structural properties of neural networks and their time-frequency characteristics simultaneously. Consequently, the combination of graph-theoretic metrics and wavelet coherence provided a powerful approach for analyzing signals in complex systems, where both network structure and temporal dynamics play crucial roles [93].

Wavelet coherence values calculated for pleasant data within each frequency band (delta, theta, alpha, and beta) and for each combination of ERP components, namely the individual components (N100, N200, P300), their pairwise concatenations (N100–N200, N100–P300, N200–P300), and the entire component (N100–N200–P300), were computed for each trial of each subject as detailed in the previous section. This was repeated for each ERP component (N100, N200, and P300) and their combinations.

Using the resulting wavelet coherence matrices across all channel pairs, adjacency matrices were constructed for each frequency band and ERP component. For example, three different adjacency matrices were created for the delta band correspond-

ing to the N100, N200, and P300 ERP components. This procedure was similarly applied for the theta, alpha, and beta bands. The same methodology was employed for the unpleasant data to produce the corresponding adjacency matrices for each frequency band and each ERP component.

After constructing adjacency matrices, a set of global and local graph-theoretic measures, which are given below, was computed to characterize the topological properties of functional brain networks. These graph metrics were derived separately for each trial in both pleasant and unpleasant datasets by using the Brain Connectivity Toolbox [111], based on the connectivity maps obtained for each ERP component and for each frequency band. The computed metrics were used as features for subsequent analysis, aiming to distinguish between the two emotional states by capturing differences in brain network organization across each frequency band and ERP component.

- energy of the graph.
- characteristic path length of the graph.
- global efficiency of the graph.
- clustering coefficient of the graph.
- strength of the graph.
- transitivity of the graph.

Each graph-theoretic metric was computed independently for every combination of ERP component, namely the individual windows (N100, N200, P300), their pairwise concatenations (N100–N200, N100–P300, N200–P300), and the entire component (N100–N200–P300), in each frequency band. For example, energy of the graph was estimated separately for the N100, N200, and P300 intervals and their combinations, and this analysis was repeated for the delta, theta, alpha, and beta bands.

After global and local graph-theoretic metrics were derived from the original graphs, identical computation was conducted on 100 surrogate graphs. The threshold values were selected heuristically in accordance with previous work [111],[123] as there is no universally accepted thresholding criterion. Specifically, proportional threshold levels of 0.1, 0.2, and 0.3 were applied during surrogate-graph construction. These sparsity levels were chosen because the brain network usually was within this range [1]. Following the computation of graph metrics for both the original and surrogate graphs, each measure was normalized via $z$-score normalization; the mean value of each surrogate parameter was subtracted from the original value and divided by its standard deviation.

Two local metrics, namely, the strength and clustering coefficient, were computed for each of the 30 channels, while four global metrics, namely, energy, global efficiency, transitivity, and characteristic path length, were extracted for the entire network, yielding 2 x 30 + 4 = 64 features per trial. Feature selection was conducted via three different approaches. First, the $t$-test was applied to each feature across the two classes. Second, the ReliefF algorithm [61],[151],[96] was used, and the top 20 most discriminative features were selected for classification. For comparison, the minimum-redundancy maximum-relevance (MRMR) criterion was also evaluated but proved less effective than either the ReliefF or the $t$-test. Therefore, the classification result via MRMR feature selection was not presented in this thesis. Classification was performed separately within the delta, theta, alpha, and beta bands using k-nearest neighbors (k-NN), linear discriminant analysis (LDA), and support vector machines (SVM). A 10-fold cross-validation scheme, repeated 100 times, was implemented on a within-subject basis, such that each subject's trials were splitted into training and test folds. The SVM employed a radial basis-function kernel with the scale parameter fixed at one, and Bayesian optimization was adopted for hyper-parameter tuning. Fisher's LDA was used with regularisation parameters set to zero in the LDA classifier. For k-NN, Euclidean distance and a single neighbor ($k = 1$) were selected with uniform distance weighting. Within each frequency band, feature subsets derived from individual ERP components (N100, N200, and P300) and their pairwise combination (N100–N200, N100–P300, N200–P300) and three-way combination (N100–N200–P300)

were used independently. The complete analysis pipeline is shown in Figure 4.20.

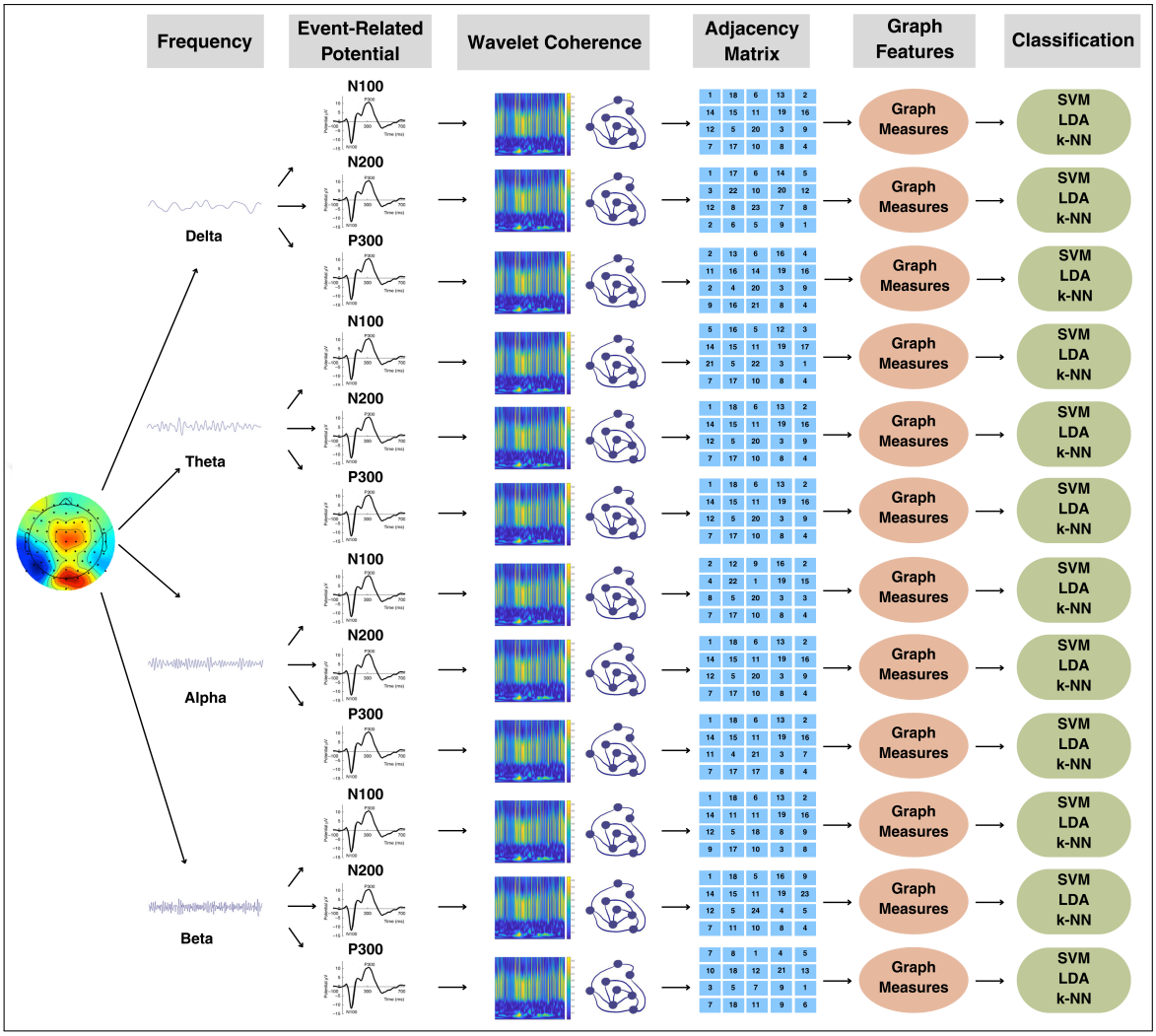


**Figure 4.20** Graph measures based classification pipeline.

A comprehensive evaluation across all frequency bands showed that theta, alpha, and beta band classifiers did not surpassed 65% accuracy for any subject in either dataset. Accordingly, subsequent analysis focused on the delta band, which exhibited the greatest discriminative performance. Optimal performance was obtained when the delta band features corresponding to the three-way combination of ERP components (N100–N200–P300) were selected using either the *t*-test or the ReliefF algorithm by applying the SVM classifier. Subject-level SVM classification accuracies by applying the *t*-test feature selection and the ReliefF algorithm are summarized in Table 4.2 and Table 4.3, respectively. The classification results are averaged over 100 iterations of ten-fold cross-validation, and the reported results correspond to the mean computed across

the 100 repeated cross-validation iterations. With the *t*-test feature selection, the mean accuracy across subjects reached 89.9% and the maximum classification performance of 96.1% achieved for Subject-5, as shown in Table 4.2.

**Table 4.2**
SVM classification performance for each subject by using N100, N200, and P300 delta band graph features selected with the *t*-test method.

| *t*-test | Accuracy(%) | Sensitivity(%) | Specificity(%) | F1 Score(%) |
|---|---|---|---|---|
| Subject-1 | 87.5 | 89.0 | 86.1 | 87.9 |
| Subject-2 | 87.3 | 89.1 | 85.4 | 87.6 |
| Subject-3 | 92.4 | 95.1 | 89.6 | 92.6 |
| Subject-4 | 84.6 | 85.2 | 84.3 | 84.9 |
| Subject-5 | 96.1 | 96.7 | 95.5 | 96.2 |
| Subject-6 | 91.0 | 92.8 | 89.1 | 91.2 |
| Subject-7 | 90.7 | 92.2 | 89.4 | 90.9 |
| Subject-8 | 88.3 | 83.5 | 93.4 | 87.9 |
| Subject-9 | 91.1 | 91.9 | 90.4 | 91.2 |
| Subject-10 | 91.2 | 90.1 | 92.4 | 91.2 |
| Subject-11 | 84.3 | 81.5 | 86.8 | 83.8 |
| Subject-12 | 93.0 | 91.5 | 94.6 | 92.9 |
| Subject-13 | 91.6 | 95.8 | 87.2 | 91.8 |
| Average | 89.9 | 90.3 | 89.6 | 90.0 |

According to Table 4.3, the ReliefF method further raised the mean to 91.8% and the maximum classification performance of 96.5% achieved again for Subject-5.

**Table 4.3**
SVM classification performance for each subject by using N100, N200, and P300 delta band graph features selected with the ReliefF method.

| ReliefF | Accuracy(%) | Sensitivity(%) | Specificity(%) | F1 Score(%) |
|---|---|---|---|---|
| Subject-1 | 91.9 | 92.4 | 90.5 | 91.6 |
| Subject-2 | 90.7 | 90.6 | 88.6 | 89.8 |
| Subject-3 | 93.2 | 94.2 | 91.4 | 92.9 |
| Subject-4 | 89.8 | 91.9 | 88.6 | 90.4 |
| Subject-5 | 96.5 | 97.7 | 94.0 | 96.0 |
| Subject-6 | 91.1 | 89.7 | 90.2 | 90.0 |
| Subject-7 | 93.0 | 93.1 | 91.6 | 92.4 |
| Subject-8 | 90.6 | 88.9 | 93.4 | 91.0 |
| Subject-9 | 91.5 | 92.7 | 90.6 | 91.8 |
| Subject-10 | 89.5 | 88.4 | 90.7 | 89.5 |
| Subject-11 | 90.4 | 89.2 | 92.9 | 90.9 |
| Subject-12 | 95.7 | 94.6 | 96.0 | 95.3 |
| Subject-13 | 92.3 | 95.0 | 90.2 | 92.8 |
| Average | 91.8 | 92.2 | 91.4 | 91.9 |

# 5. COGNITIVE DATA ANALYSIS AND RESULTS

The cognitive dataset was examined using a methodological framework and processing pipeline similar to the emotional data. This chapter provides a comprehensive overview of each analytical step.

## 5.1 Preprocessing

EEG data has been taken with a sample rate of 1 kHz. via 63 channels (Fp1, Fp2, AF7, AF3, AF4, AF8, F9, F7, F5, F3, F1, Fz, F2, F4, F6, F8, F10, FT7, FC5, FC3, FC1, FCz, FC2, FC4, FC6, FT8, C5, C3, C1, Cz, C2, C4, C6, T8, TP7, CP5, CP3, CP1, CPz, CP2, CP4, CP6, TP8, P9, P7, P5, P3, P1, Pz, P2, P4, P6, P8, P10, PO7, PO3, POz, PO4, PO8, O1, Oz, O2, EOG) and then it was down sampled into 100 Hz. The EEG signals were re-referenced to the left (A2) and right (Ref) mastoid channels. After eliminating the EOG channel, the signal was band-pass filtered with a zero-phase, non-causal FIR filter (order = 43; pass-band edge = 32 Hz.; –6 dB cutoff = 36 Hz.) [29]. Then, 1 Hz. FIR filter of order 300 was used, using least-squares error minimization and reverse digital filtering with zero-phase effect. A 50 Hz. notch filter was used for line noise supression.

Channels with a variance of less than 0.5 in more than 10% of the trials were removed. Furthermore, epochs containing muscle artifacts were also eliminated, characterized by excessive variance in more than 20% of the channels. A max-min criterion was applied and epochs having more than 150 $\mu$V difference between maximum and minimum voltage in channels (F9, F10, AF3, AF4) to get rid of eye movement artifacts [97]. Independent Component Analysis (ICA) with artifactual component selection given by the Multiple Artifact Rejection Algorithm (MARA) [145] was applied for removing the artifact data, including smaller eye movement artifacts, muscular artifacts, and loose electrodes. In addition to this, visual inspection was performed on each ICA component by considering the power spectral density and its topographic distribution.

EEG data were segmented into epochs according to the timing, as shown in Figure 3.5. EEG data were segmented into epochs comprising a 500 ms pre-stimulus fixation, followed by a 1,250 ms stimulus-presentation window, and a 750 ms rest period. To minimize background activity, each epoch was baseline corrected using the 200 ms immediately preceding stimulus onset.

## 5.2 ERP Analysis

After obtaining epochs for two distinct cognitive tasks across all subjects, ERP analysis was performed to determine whether there were differences between low and high cognitive states. The grand averages of the ERPs were obtained by averaging across all of the trials and subjects for two different tasks. In this way, it was aimed to determine whether neurophysiological differences in the subjects' responses to two different cognitive tasks can be observed. The grand averages across all subjects and trials, for each task are shown in Figure 5.1, Figure 5.2, Figure 5.3, Figure 5.4, Figure 5.5, and Figure 5.6, respectively. Since the biggest differences between two cognitive tasks have been observed in the Fz, F3, F4, Cz, C3 and Pz channels, only the ERPs associated with these channels have been presented. Grand-average ERPs across all subjects and trials reveal clear distinctions between low and high level cognitive states within the N100, N200, and P300 ERP components as in the figures.

In emotional data, a two-stage procedure was employed: calculation of wavelet coefficients of each ERP component, followed by wavelet coherence computation to obtain graph-theoretic metrics. However, the initial step—wavelet decomposition—was omitted in the cognitive condition due to the modest classification results obtained in the emotional data. Instead, wavelet coherence was directly calculated on the ERP components, as the main focus was on connectivity based graph metrics rather than in the absolute values of the wavelet coefficients.

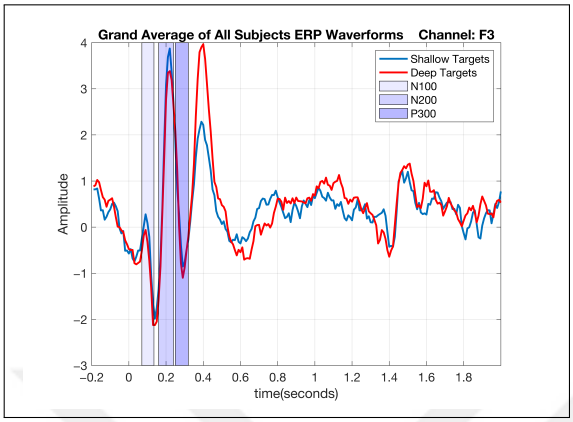


**Figure 5.1** ERP waveform of F3 channel.

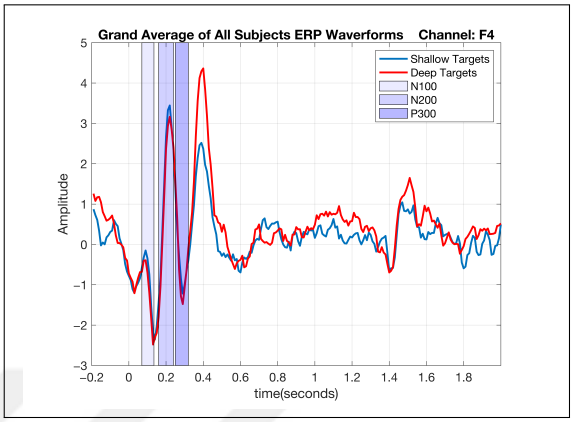


**Figure 5.2** ERP waveform of F4 channel.

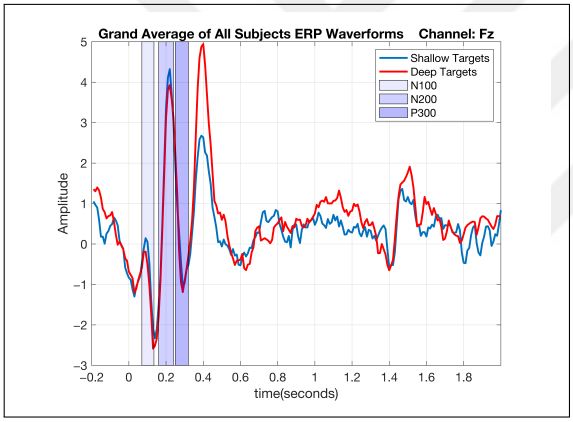


**Figure 5.3** ERP waveform of Fz channel.

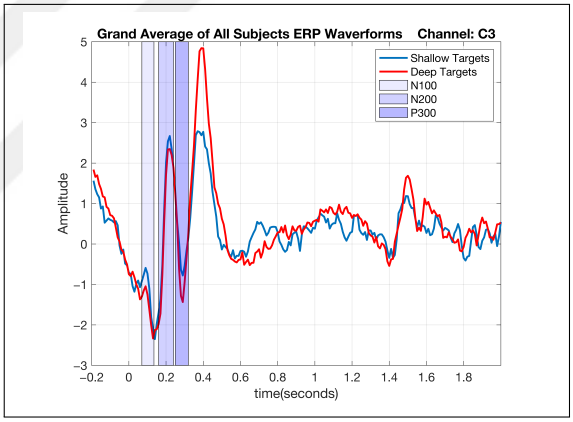


**Figure 5.4** ERP waveform of C3 channel.

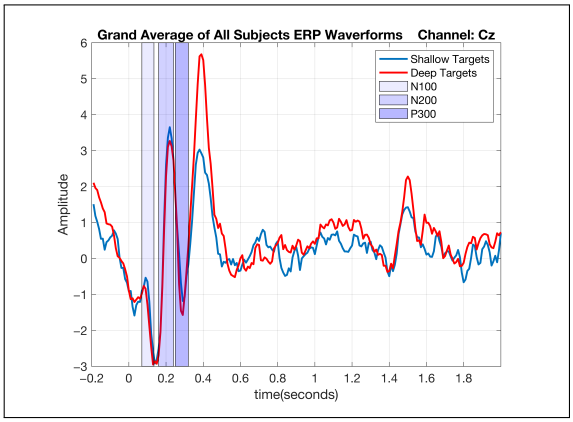


**Figure 5.5** ERP waveform of Cz channel.

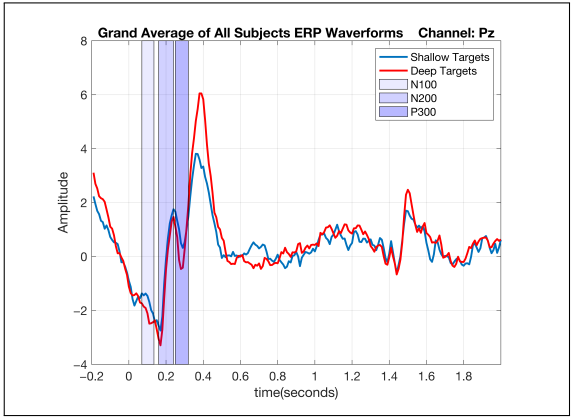


**Figure 5.6** ERP waveform of Pz channel.

## 5.3 Wavelet Coherence Analysis

The same procedure applied to processing the emotional data was also employed for the cognitive data. Wavelet coherence values associated with the N100, N200, and P300 ERP components for low and high cognitive states were calculated for 62 channels in the delta, theta, alpha, and beta frequency bands. Later, considering wavelet coherence values among all channels of EEG data (low & high cognitive states) it was investigated whether there was a difference between two different states in each ERP component. The connectivity map showing the differences in wavelet coherence values between low and high cognitive states for the N100 ERP component was obtained, as shown in Figure 5.7. EEG channels, namely Fp1, Fp2, AF7, AF3, AF4, AF8, F9, F7, F5, F3, F1, Fz, F2, F4, F6, F8, F10, FT7, FC5, FC3, FC1, FCz, FC2, FC4, FC6, FT8, C5, C3, C1, Cz, C2, C4, C6, T8, TP7, CP5, CP3, CP1, CPz, CP2, CP4, CP6, TP8, P9, P7, P5, P3, P1, Pz, P2, P4, P6, P8, P10, PO7, PO3, POz, PO4, PO8, O1, Oz, O2, were numbered from 1 to 62 on both axes. Lighter hues indicate larger differences, whereas darker hues denote smaller ones in the figures.

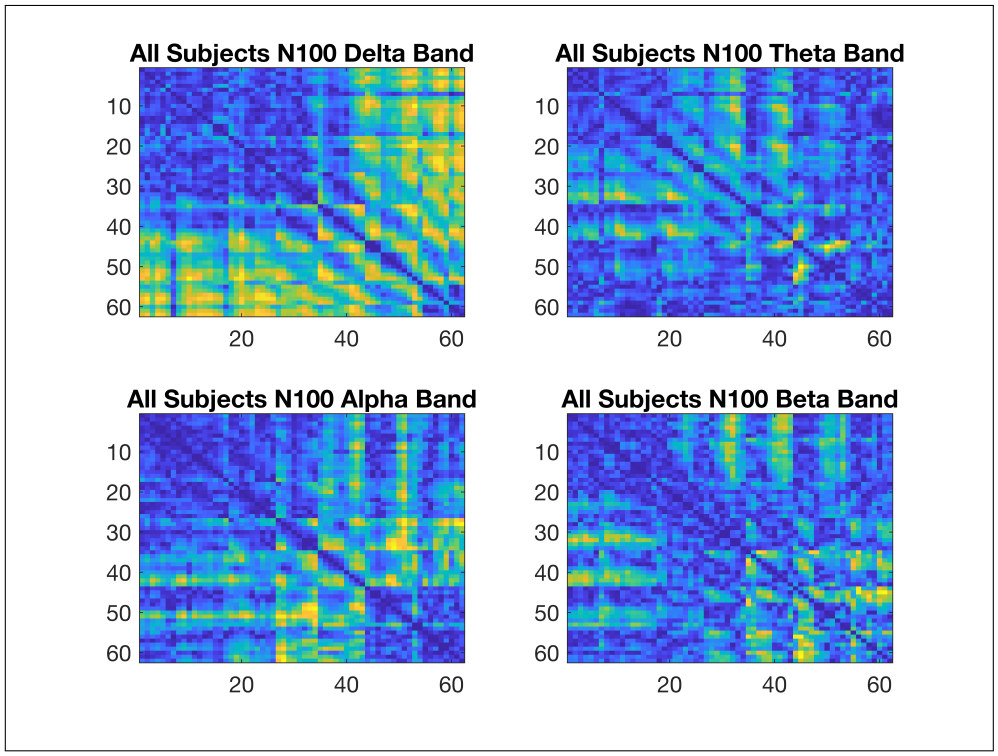


**Figure 5.7** N100 connectivity maps of difference for delta, theta, alpha, and beta frequency bands.

Wavelet coherence difference maps for low and high cognitive states corresponding to the N200 and P300 components were also plotted, as seen in Figure 5.8 and Figure 5.9, respectively.

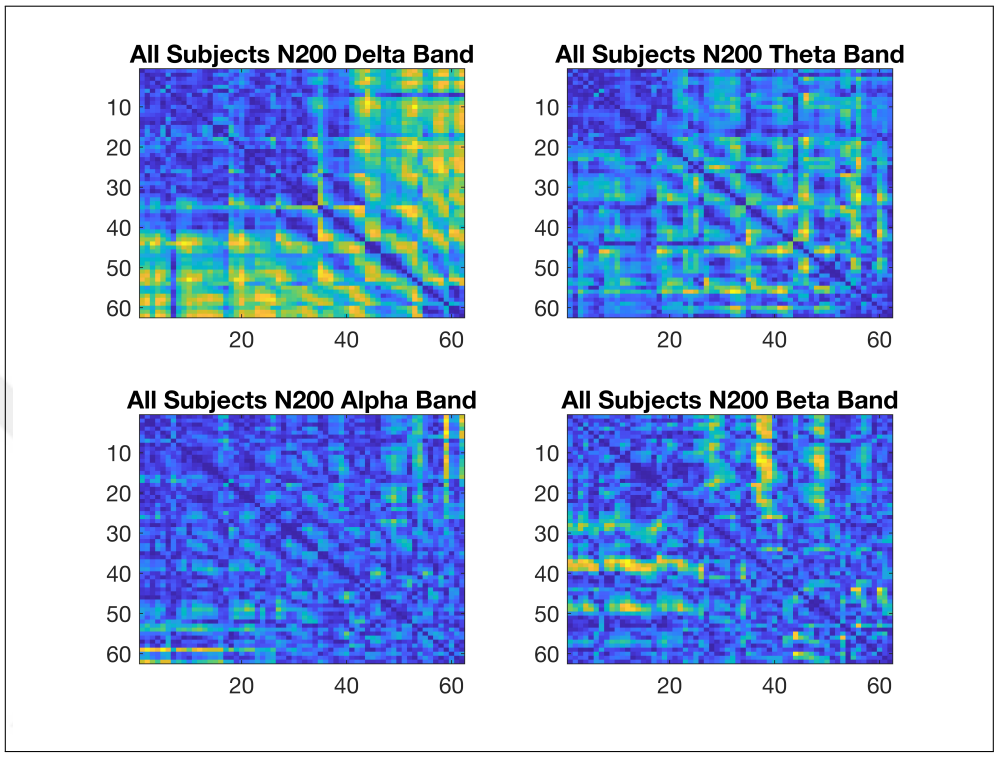


**Figure 5.8** N200 connectivity maps of difference for delta, theta, alpha, and beta frequency bands.

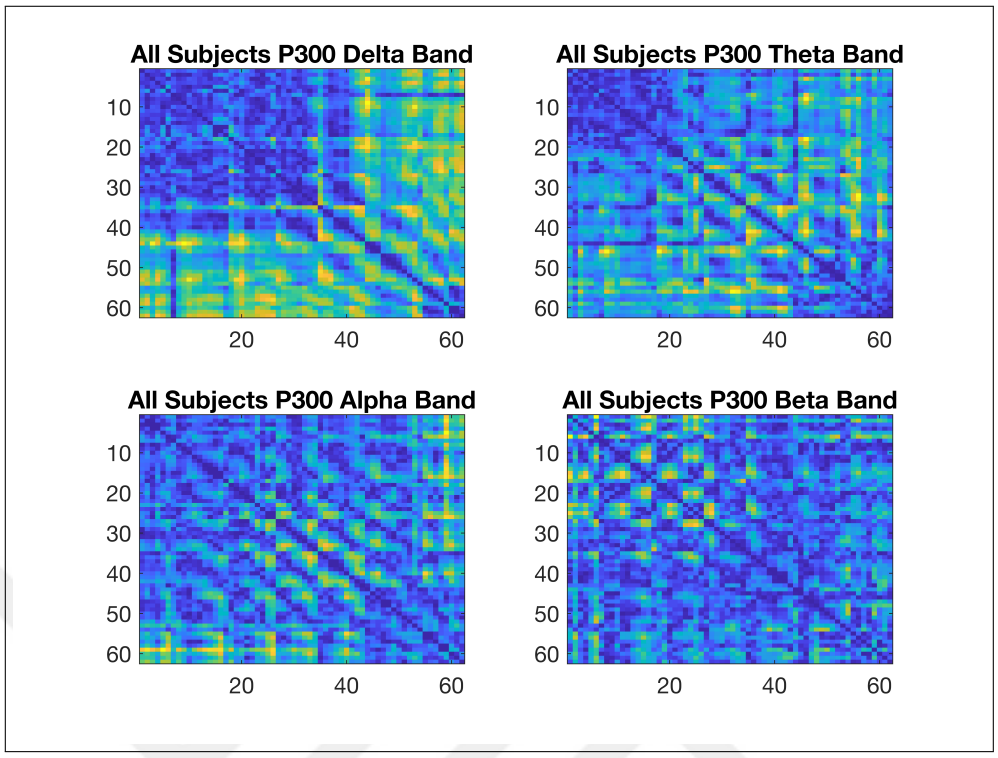


**Figure 5.9** P300 connectivity maps of difference for delta, theta, alpha, and beta frequency bands.

## 5.4 Graph-Theoretic Metrics

The same feature extraction and feature selection methods employed for the classification of the emotional data, as described in Section 4.5, were also applied to the cognitive data.

As one of the feature selection methods, the *t*-test was applied to each feature across the two classes, namely low  high cognitive states. Furthermore, the ReliefF method was applied to select the top 10 most discriminative features to be used in the classification stage. The k-NN, LDA, and SVM classifiers were used to discriminate low and high cognitive states in the delta, theta, alpha, and beta frequency bands. Each ERP component and their combination were considered during the classification. Thus, feature sets were formed using individual ERP components (N100, N200, and P300) and their pairwise combinations (N100–N200, N100–P300, N200–P300) and three-way

combination (N100–N200–P300). The classification process was implemented using 10-fold cross-validation and was conducted 100 times to ensure robustness, and the reported results represent the average over these 100 iterations. It was implemented on a within-subject basis, such that each subject's trials were splitted into training and test folds.

The highest classification rate was achieved with the SVM classifier when the features corresponding to the three-way combination of ERP components (N100–N200–P300) in the delta band. The SVM classification results by using the *t*-test feature selection obtained for each subject are given in Table 5.1. According to the classification results using the *t*-test method, an average classification performance of 83.5% was observed across the subjects, with the maximum classification performance of 93.6% achieved for Subject 5.

**Table 5.1**
SVM classification performance for each subject by using N100, N200, and P300 delta band graph features selected with the *t*-test method.

| *t*-test | Accuracy(%) | Sensitivity(%) | Specificity(%) | F1 Score(%) |
|---|---|---|---|---|
| Subject-1 | 82.4 | 81.7 | 83.3 | 82.6 |
| Subject-2 | 87.4 | 89.5 | 85.5 | 87.9 |
| Subject-3 | 90.4 | 92.7 | 88.5 | 90.9 |
| Subject-4 | 89.9 | 89.1 | 90.7 | 89.9 |
| Subject-5 | 93.6 | 95.0 | 92.1 | 93.7 |
| Subject-6 | 88.6 | 88.6 | 88.0 | 88.5 |
| Subject-7 | 91.6 | 89.9 | 93.4 | 91.6 |
| Subject-8 | 69.2 | 71.4 | 70.2 | 70.9 |
| Subject-9 | 80.0 | 82.3 | 83.1 | 80.3 |
| Subject-10 | 75.6 | 77.0 | 78.1 | 76.2 |
| Subject-11 | 78.8 | 80.2 | 81.0 | 79.8 |
| Subject-12 | 75.2 | 77.4 | 76.5 | 76.1 |
| Subject-13 | 73.1 | 75.2 | 74.7 | 74.1 |
| Subject-14 | 87.9 | 86.3 | 89.2 | 87.7 |
| Subject-15 | 88.4 | 82.5 | 94.4 | 87.8 |
| Average | 83.5 | 83.9 | 84.6 | 83.9 |

When the ReliefF method was chosen for feature selection, an average classification performance of 88.5% was observed across the subjects, with a maximum classification performance of 92.2% achieved for Subject 5. Subject-level SVM classification accuracies with the sensitivity, specificity, and F1 scores are presented in Table 5.2.

**Table 5.2**
SVM classification performance for each subject by using N100, N200, and P300 delta band graph features selected with the ReliefF method.

| ReliefF | Accuracy(%) | Sensitivity(%) | Specificity(%) | F1 Score(%) |
|---|---|---|---|---|
| Subject-1 | 90.2 | 91.0 | 89.2 | 90.3 |
| Subject-2 | 85.8 | 88.0 | 83.6 | 86.3 |
| Subject-3 | 90.8 | 91.9 | 89.6 | 91.0 |
| Subject-4 | 91.3 | 90.2 | 92.8 | 91.5 |
| Subject-5 | 92.2 | 93.3 | 90.9 | 92.3 |
| Subject-6 | 88.0 | 85.8 | 90.3 | 87.9 |
| Subject-7 | 85.8 | 85.5 | 86.2 | 86.0 |
| Subject-8 | 88.0 | 88.9 | 87.2 | 88.4 |
| Subject-9 | 87.7 | 89.1 | 86.3 | 88.1 |
| Subject-10 | 91.1 | 91.2 | 91.0 | 91.3 |
| Subject-11 | 89.0 | 88.7 | 89.7 | 89.3 |
| Subject-12 | 86.3 | 83.4 | 89.3 | 86.2 |
| Subject-13 | 87.2 | 85.4 | 89.1 | 89.6 |
| Subject-14 | 89.3 | 89.8 | 89.1 | 89.6 |
| Subject-15 | 85.2 | 85.2 | 85.2 | 85.3 |
| Average | 88.5 | 88.5 | 88.6 | 88.7 |

# 6. DISCUSSION

## 6.1 Comparison with Existing Literature

In this thesis, several local and global graph-theoretic features derived from wavelet coherence-based connectivity maps for different ERP components were investigated. The proposed approach was applied to both emotional and cognitive data. Graph-theoretic metrics obtained from wavelet coherence values were employed to classify data from the two experimental conditions. Among various EEG studies on graph-based classification in the literature, many used PLV based connectivity maps [79],[49],[142]. Some studies applied wavelet coherence values to obtain graph-theoretic measures, but did not focus on individual ERP components [119],[114]. To our knowledge, this study is the first to investigate graph-theoretic metrics across multiple frequency bands by incorporating wavelet coherence values obtained from several ERP components.

It was revealed that channels F3, F4, C3, and Cz were the most discriminative between two conditions in each dataset, which was aligned with previous studies highlighting channels F3, F4, and Fz as particularly notable in the emotional and cognitive paradigms [139],[59]. Moreover, the results obtained demonstrated that the integration of features from multiple ERP components improved the classification accuracy across both datasets. The proposed approach enhanced ST–DT discrimination performance to 88.5%, compared to the performance of around 72% reported in [97] using the same data. Classification accuracy in the delta band exceeded 90% for both the emotional and cognitive paradigms. This finding is in line with the results of another study [69], which highlighted that low frequency oscillations are closely associated with affective processes. In addition, delta band activity was shown to be associated with long-range cortico-cortical functional connectivity, which is critical for large-scale brain network communication [17]. Based on the performance of the classification in the delta band, it was concluded that the delta band connectivity patterns show considerable modulation

during the emotional and cognitive paradigms.

Using multiple ERP components yielded more promising results in the classification of emotional EEG data, which are consistent with the findings of another study that selected several ERP components in its classification analysis [108]. This emphasizes the significiance of using wavelet coherence values for the N100, N200, and P300 ERP components in combination to distinguish emotional moods. These results are in accordance with the findings of a study that demonstrated the importance of using multiple ERP components other than P300 in the recognition of facial emotions [132]. Integration of ERP components into connectivity analysis provided insight into neural activity over time in different brain regions during task execution [8] by enriching our understanding of neural processing in both emotional and cognitive paradigms. One study [148] that used the DEAP dataset combined graph-based features, derived from mutual information, with the statistical features, derived from peripheral physiological signals, classification rates of 88.3% and 90.8% were obtained for valence and arousal, respectively. In a study [142] using the SEED dataset, PLV-based graphs were used to obtain connectivity metrics and a classification of 84.4% was achieved. The same study reported average accuracies of 73.3%, 77.0%, and 79.2% for valence, arousal, and dominance classifications, respectively, based on the DEAP database. As another paradigm, motor imagery data were analyzed using graph metrics in one study [123], a classification performance of 87% was achieved, which remained below those presented in this thesis. Using varying threshold levels for surrogate graph construction did not yield large differences. Finally, the ReliefF algorithm based feature selection consistently outperformed the *t*-test method–based selection in average on both emotional and cognitive datasets.

## 6.2 Summary of Key Findings

Among all graph-theoretic metrics, the clustering coefficient parameter was found to be a discriminatory feature between the two experimental conditions in both datasets. This finding demonstrates a condition-specific reorganization of local net-

work segregation. It implies a systematic variation balance between short-range feedback connections and long-range integration between the two different classes [111]. A higher clustering coefficient in one group shows a greater density of triangular motifs among neighboring nodes, and this aligns with more closely connected, functionally specialized subnetworks designed for rapid, context-dependent information exchange [109]. This arrangement is thought to enhance both fault tolerance and processing efficiency within local circuits. Condition-dependent increases in clustering are typically associated with increased attentional demands or emotional arousal [157], whereas reduced clustering represents states that promote distributed processing or globally synchronous dynamics, such as relaxed wakefulness or certain sleep stages. Although emotional and cognitive paradigms bring comparable complexity changes in the structural features of the data, cognitive tasks typically impose greater processing demands than emotional tasks. Part of the decrease in cognitive classification over emotion may be accounted for its relative complexity and demandedness. Moreover, cognitive activities evoke overlapping neural activations, resulting in less distinct patterns than emotional activities.

Delta waves are generated by extensive, reciprocally connected cortico-subcortical loops, whose long cycle length accommodates axonal conduction delays, making them well-suited for coordinating activity across distant regions of the brain [131],[5],[95]. Studies indicate that there is an inverse relationship between spatial extent of a network and the preferred oscillatory frequency. Thus, large-scale interactions are typically observed in the delta/theta range [48]. In one study [115], it is demonstrated that the effective down-regulation of affect improves delta-band synchrony in prefrontal–limbic pathways and various other emotion networks. The same pathways facilitate cognitive control over emotional processing, offering a plausible explanation for why delta connectivity encompasses joint information about both areas in the dataset. Furthermore, delta rhythms show a higher signal-to-noise ratio in the scalp [56] and are less influenced by muscle artifacts compared to beta and gamma activity. Their slower time scale enables a more reliable estimation of phase-based connectivity, such as wavelet coherence, over the duration typically employed in emotion–cognition paradigms. Consequently, these statistical advantages give rise to the generation of cleaner adjacency

matrices, yielding more distinct graph-theoretic features. In agreement with the findings of this thesis about clustering coefficients for emotional data, one study [109] reported on the clustering coefficient discrimination among different emotions based on connectivity in the delta band. Similarly, another study [157] observed clustering coefficient discrimination between two different cognitively demanding tasks, in line with the results presented in this thesis. These observations highlight the predominance of delta band connectivity for classification and suggest that adaptive brain–computer interfaces should emphasize slow frequency graph metrics features especially when user states are affected by a combination of emotional and cognitive factors.

After assessing the classification results across all subjects in both paradigms, the findings confirm that variations in cognitive load and pleasant versus unpleasant emotional moods can be classified with high success rates using the SVM classifier after deriving graph-theoretic metrics based on wavelet coherence values in certain frequency bands of ERP components. The framework proposed in this thesis could potentially be applied to different types of EEG data.

# 7. CONCLUSION

## 7.1 Limitations of the Study

Some limitations in this thesis can be addressed. First, increasing the number of subjects to improve the statistical power is certainly a significant aspect in such a study. Nonetheless, the classification approach focused on individual subjects whose datasets contained more than 500 trials each, used for both training and testing. The classification rates for through 13 (15) subjects did not vary by a margin of more than 7% percent, as presented in Table 4.2, 4.3, 5.1, and 5.2. Thus, a certain level of consistency in classification performance was achieved across subjects, even though the subjects represent a larger group also encountered in similar studies in the literature [126],[83],[153],[64]. A main limitation of current BCI systems is their requirement for subject-specific calibration, and optimal performance can only be reached by training the system individually for each user. Furthermore, EEG data were recorded from each subject in one session only. Even if this issue is compatible with existing EEG-based studies, the validity of the results and the reliability of the measurement could be improved by using data collected over multiple sessions to account for variability due to biorhythms. To cope with these limitations, multiple sessions of individual data collection would enhance the training performance of the BCI systems. In addition, emotional responses may vary as a result of sociological and cultural differences [148]. Emotional data could be obtained from people raised in different cultural settings to reduce the effects of such variability. Lastly, the basis for the analysis of emotional and cognitive data could be augmented to other types of physiological signals [65], such as electrocardiography, electro-dermal activity, blood pressure, heart rate, and respiration.

## 7.2 Future Directions

BCI technology remains a challenging yet futuristic research area with humanity still at the early stages of exploration. Graph-theoretic metrics based on wavelet coherence gave promising results in the discrimination of emotional moods and cognitive states. Hence, future studies can focus on that direction of research. Moreover, the applicability of this proposed method can be extended to other types of data, such as motor imagery or inner reading. The results obtained imply that the proposed method is a viable approach to understanding and investigating emotional and cognitive states under different conditions using EEG data. A promising direction for subsequent research is the development of integrated neurofeedback protocols that synchronously modulate emotional and cognitive processes. The rigorous design and evaluation of such designs could be beneficial in geriatric and educational methods in addition to neurofeedback applications.

## 7.3 Proceedings and Articles During Thesis

1. Application of graph-theoretic methods using ERP components and wavelet coherence on emotional and cognitive EEG data, Deniz, S. M., Ademoglu, A., Duru, A. D., Demiralp, T. (2025), *Brain Sciences*, 15(7), 714.

2. Measuring the effect of mental workload and explanations on appropriate AI reliance using EEG, Zhang, Z. T., Argın, S. K., Bilen, M. B., Urgun, D., Deniz, S. M., Liu, Y., Hassib, M. (2024), *Behaviour Information Technology*, 1-19, https://doi.org/10.1080/0144929X.2024.2431055.

3. Prediction of lifted weight category using EEG equipped headgear, Deniz, S.M., Javaheri, H., Vargas, J.F., Urgun, D., Sabit, F., Tok, M., Haklidir, M., Zhou, B. and Lukowicz, P. (2022, September), *In 2022 IEEE-EMBS International Conference on Biomedical and Health Informatics (BHI)*, (pp. 1-7). IEEE. doi:10.1109/BHI56158.2022.9926744.

4. ERP based wavelet analysis for emotion classification, Deniz, S. M., Kurt E., Duru A. D., Demiralp, T., Ademoğlu, A. *National Neuroscience Conference, USK 2018 Proceedings*, İstanbul Technical University, İstanbul, pp 152, 20-23 May 2018.

5. Changes in ongoing EEG rhythms in response to dynamic visual stimuli with different emotional valence and arousal levels, Erbey, M., Deniz, S. M., Demiralp, T. (2014, June). *In 20th Annual Meeting of the Organization for Human Brain Mapping (OHBM).*

6. Emotion recognition based on spatially smooth spectral features of the EEG, Balli, T., Deniz, S. M., Cebeci, B., Erbey, M., Duru, A. D., Demiralp, T. (2013, November), *In 2013 6th International IEEE/EMBS Conference on Neural Engineering (NER)*, (pp. 407-410). IEEE.

# Bibliography


[1] Sophie Achard and Ed Bullmore. "Efficiency and cost of economical brain functional networks". In: *PLoS Computational Biology* 3.2 (2007), e17.

[2] A Ademoglu et al. "Decomposition of event-related brain potentials into multicomponents using wavelet transform". In: *Applied Signal Processing* 5.3 (1998), pp. 142–151.

[3] Ahmet Ademoglu, Evangelia Micheli-Tzanakou, and Yorgo Istefanopoulos. "Analysis of pattern reversal visual evoked potentials (PRVEPs) by spline wavelets". In: *IEEE Transactions on Biomedical Engineering* 44.9 (1997), pp. 881–890.

[4] Mehmet Akin. "Comparison of wavelet transform and FFT methods in the analysis of EEG signals". In: *Journal of Medical Systems* 26 (2002), pp. 241–247.

[5] Mohammad Aliramezani et al. "Delta-alpha/beta coupling as a signature of visual working memory in the prefrontal cortex". In: *Iscience* 27.8 (2024).

[6] Pietro Aricò et al. "A passive brain–computer interface application for the mental workload assessment on professional air traffic controllers during realistic air traffic control tasks". In: *Progress in Brain Research* 228 (2016), pp. 295–328.

[7] Sima Azizi, Daniel B Hier, and Donald C Wunsch. "Schizophrenia classification using resting state EEG functional connectivity: source level outperforms sensor level". In: *2021 43rd Annual International Conference of the IEEE Engineering in Medicine & Biology Society (EMBC)*. IEEE. 2021, pp. 1770–1773.

[8] Jang-Han Bae et al. "Connectivity changes in two-channel prefrontal ERP associated with early cognitive decline in the elderly population: beta band responses to the auditory oddball stimuli". In: *Frontiers in Aging Neuroscience* 16 (2024), p. 1456169.

[9] Mohamad Amin Bakhshali et al. "Coherence-based correntropy spectral density: A novel coherence measure for functional connectivity of EEG signals". In: *Measurement* 140 (2019), pp. 354–364.

[10] Tugce Balli et al. "Emotion recognition based on spatially smooth spectral features of the EEG". In: *2013 6th International IEEE/EMBS Conference on Neural Engineering (NER)*. IEEE. 2013, pp. 407–410.

[11] Erol Basar et al. "Oscillatory brain dynamics, wavelet analysis, and cognition". In: *Brain and Language* 66.1 (1999), pp. 146–183.

[12] Merve Dogruyol Basar, Adil Deniz Duru, and Aydin Akan. "Emotional state detection based on common spatial patterns of EEG". In: *Signal, Image and Video Processing* 14.3 (2020), pp. 473–481.

[13] E rol Başar et al. "Event-related oscillations are 'real brain responses'—wavelet analysis and new strategies". In: *International Journal of Psychophysiology* 39.2-3 (2001), pp. 91–127.

[14] Magali Batty and Margot J Taylor. "Early processing of the six basic facial emotional expressions". In: *Cognitive Brain Research* 17.3 (2003), pp. 613–620.

[15] Edward Bernat, Scott Bunce, and Howard Shevrin. "Event-related brain potentials differentiate positive and negative mood adjectives during both supraliminal and subliminal visual processing". In: *International Journal of Psychophysiology* 42.1 (2001), pp. 11–34.

[16] Benjamin Blankertz et al. "Single-trial analysis and classification of ERP components—a tutorial". In: *NeuroImage* 56.2 (2011), pp. 814–825.

[17] Pierre Bourdillon et al. "Brain-scale cortico-cortical functional connectivity in the delta-theta band is a robust signature of conscious states: an intracranial and scalp EEG study". In: *Scientific Reports* 10.1 (2020), p. 14037.

[18] M Bradley and PJ Lang. *Emotion and motivation. cacioppo Jt, tassinary lG, Berntson G (eds) handbook of psychophysiology.* 2007.

[19] Anne-Marie Brouwer et al. “Monitoring mental state during real life office work”. In: *Symbiotic Interaction: 6th International Workshop, Symbiotic 2017, Eindhoven, The Netherlands, December 18–19, 2017, Revised Selected Papers 6*. Springer. 2018, pp. 18–29.

[20] Ed Bullmore and Olaf Sporns. “Complex brain networks: graph theoretical analysis of structural and functional systems”. In: *Nature Reviews Neuroscience* 10.3 (2009), pp. 186–198.

[21] Christian Cajochen et al. “Daytime melatonin administration enhances sleepiness and theta/alpha activity in the waking EEG”. In: *Neuroscience Letters* 207.3 (1996), pp. 209–213.

[22] Cinzia Cecchetto et al. “Emotional reactions in moral decision-making are influenced by empathy and alexithymia”. In: *Social Neuroscience* 13.2 (2018), pp. 226–240.

[23] Guillaume Chanel et al. “Emotion assessment: Arousal evaluation using EEG’s and peripheral physiological signals”. In: *International Workshop on Multimedia Content Representation, Classification and Security*. Springer. 2006, pp. 530–537.

[24] Duo Chen et al. “A high-performance seizure detection algorithm based on Discrete Wavelet Transform (DWT) and EEG”. In: *PloS One* 12.3 (2017), e0173138.

[25] Giovanni Chiarion et al. “Connectivity analysis in EEG data: a tutorial review of the state of the art and emerging trends”. In: *Bioengineering* 10.3 (2023), p. 372.

[26] Samy Chikhi, Nadine Matton, and Sophie Blanchet. “EEG power spectral measures of cognitive workload: A meta-analysis”. In: *Psychophysiology* 59.6 (2022), e14009.

[27] Antonio R Damasio. “Descartes’ Error: Emotion, Reason, and the Human Brain”. In: *Grosset/Putnam* (1994).

[28] Richard J Davidson and Nathan A Fox. “Asymmetrical brain activity discriminates between positive and negative affective stimuli in human infants”. In: *Science* 218.4578 (1982), pp. 1235–1237.

[29] Arnaud Delorme and Scott Makeig. “EEGLAB: an open source toolbox for analysis of single-trial EEG dynamics including independent component analysis”. In: *Journal of Neuroscience Methods* 134.1 (2004), pp. 9–21.

[30] Tamer Demiralp and Ahmet Ademoglu. “Decomposition of event-related brain potentials into multiple functional components using wavelet transform”. In: *Clinical Electroencephalography* 32.3 (2001), pp. 122–138.

[31] Tamer Demiralp and Erol Başar. “Theta rhythmicities following expected visual and auditory targets”. In: *International Journal of Psychophysiology* 13.2 (1992), pp. 147–160.

[32] Tamer Demiralp et al. “Time–frequency analysis of single-sweep event-related potentials by means of fast wavelet transform”. In: *Brain and Language* 66.1 (1999), pp. 129–145.

[33] Tamer Demiralp et al. “Wavelet analysis of P3a and P3b”. In: *Brain Topography* 13 (2001), pp. 251–267.

[34] Gianluca Di Flumeri et al. “On the use of cognitive neurometric indexes in aeronautic and air traffic management environments”. In: *Symbiotic Interaction: 4th International Workshop, Symbiotic 2015, Berlin, Germany, October 7-8, 2015, Proceedings 4*. Springer. 2015, pp. 45–56.

[35] Shanshan Dong et al. “Individual differences in working memory capacity are reflected in different ERP and EEG patterns to task difficulty”. In: *Brain Research* 1616 (2015), pp. 146–156.

[36] Seth Duncan and Lisa Feldman Barrett. “Affect is a form of cognition: A neurobiological analysis”. In: *Cognition and Emotion* 21.6 (2007), pp. 1184–1211.

[37] Hillary Anger Elfenbein and Nalini Ambady. “Predicting workplace outcomes from the ability to eavesdrop on feelings.” In: *Journal of Applied Psychology* 87.5 (2002), p. 963.

[38] Emel Erdogdu et al. “Measurement of cognitive dynamics during video watching through event-related potentials (ERPs) and oscillations (EROs)”. In: *Cognitive Neurodynamics* 13 (2019), pp. 503–512.

[39] Giorgio Fagiolo. "Clustering in complex directed networks". In: *Physical Review E—Statistical, Nonlinear, and Soft Matter Physics* 76.2 (2007), p. 026107.

[40] Fabrizio De Vico Fallani et al. "A graph-theoretical approach in brain functional networks. Possible implications in EEG studies". In: *Nonlinear Biomedical Physics*. Vol. 4. Springer. 2010, pp. 1–13.

[41] Oliver Faust et al. "Wavelet-based EEG processing for computer-aided seizure detection and epilepsy diagnosis". In: *Seizure* 26 (2015), pp. 56–64.

[42] Andrew A Fingelkurts, Alexander A Fingelkurts, and Seppo Kähkönen. "Functional connectivity in the brain—is it an elusive concept?" In: *Neuroscience & Biobehavioral Reviews* 28.8 (2005), pp. 827–836.

[43] Nickolaos Fragopanagos and John G Taylor. "Emotion recognition in human–computer interaction". In: *Neural Networks* 18.4 (2005), pp. 389–405.

[44] Christos A Frantzidis et al. "Toward emotion aware computing: an integrated approach using multichannel neurophysiological recordings and affective visual stimuli". In: *IEEE Transactions on Information Technology in Biomedicine* 14.3 (2010), pp. 589–597.

[45] S Ganorkar and V Raut. "Comparative analysis of mother wavelet selection for EEG signal application to motor imagery based brain-computer interface". In: *Int. J. Sci. Technol. Res* 8.12 (2019), pp. 1001–1007.

[46] Carl M Gaspar, Guillaume A Rousselet, and Cyril R Pernet. "Reliability of ERP and single-trial analyses". In: *NeuroImage* 58.2 (2011), pp. 620–629.

[47] G Gaurav, Radhey Shyam Anand, and Vinod Kumar. "EEG based cognitive task classification using multifractal detrended fluctuation analysis". In: *Cognitive Neurodynamics* 15.6 (2021), pp. 999–1013.

[48] Andre Gómez-Lombardi et al. "The cognitive triad network-oscillation-behaviour links individual differences in EEG theta frequency with task performance and effective connectivity". In: *Scientific Reports* 14.1 (2024), p. 21482.

[49] Venkateswarlu Gonuguntla, Y Wang, and Kalyana C Veluvolu. "Phase synchrony in subject-specific reactive band of EEG for classification of motor imagery tasks". In: *2013 35th Annual International Conference of the IEEE Engineering in Medicine and Biology Society (EMBC)*. IEEE. 2013, pp. 2784–2787.

[50] Robert E Greenblatt, ME Pflieger, and AE Ossadtchi. "Connectivity measures applied to human brain electrophysiological data". In: *Journal of Neuroscience Methods* 207.1 (2012), pp. 1–16.

[51] David Grimes et al. "Feasibility and pragmatics of classifying working memory load with an electroencephalograph". In: *Proceedings of the SIGCHI Conference on Human Factors in Computing Systems*. 2008, pp. 835–844.

[52] Aslak Grinsted, John C Moore, and Svetlana Jevrejeva. "Application of the cross wavelet transform and wavelet coherence to geophysical time series". In: *Nonlinear Processes in Geophysics* 11.5/6 (2004), pp. 561–566.

[53] Ivan Gutman and Boris Furtula. "Graph energies and their applications". In: *Bulletin (Académie Serbe des Sciences et des Arts. Classe des Sciences Mathématiques et Naturelles. Sciences Mathématiques)* 44 (2019), pp. 29–45.

[54] Stelios K Hadjidimitriou and Leontios J Hadjileontiadis. "EEG-based classification of music appraisal responses using time-frequency analysis and familiarity ratings". In: *IEEE Transactions on Affective Computing* 4.2 (2013), pp. 161–172.

[55] Eddie Harmon-Jones, Cindy Harmon-Jones, and Elizabeth Summerell. "On the importance of both dimensional and discrete models of emotion". In: *Behavioral Sciences* 7.4 (2017), p. 66.

[56] Jeremy Harper, Stephen M Malone, and William G Iacono. "Theta-and delta-band EEG network dynamics during a novelty oddball task". In: *Psychophysiology* 54.11 (2017), pp. 1590–1605.

[57] Markus J Hofmann et al. “Affective processing within 1/10th of a second: High arousal is necessary for early facilitative processing of negative but not positive words”. In: *Cognitive, Affective, & Behavioral Neuroscience* 9 (2009), pp. 389–397.

[58] Lina Elsherif Ismail and Waldemar Karwowski. “A graph theory-based modeling of functional brain connectivity based on EEG: a systematic review in the context of neuroergonomics”. In: *IEEE Access* 8 (2020), pp. 155103–155135.

[59] Narendra Jadhav, Ramchandra Manthalkar, and Yashwant Joshi. “Effect of meditation on emotional response: An EEG-based study”. In: *Biomedical Signal Processing and Control* 34 (2017), pp. 101–113.

[60] Soobeom Jang, Seong-Eun Moon, and Jong-Seok Lee. “Graph signal representation of eeg for graph convolutional neural network”. In: (2018).

[61] A Franklin Alex Joseph and C Govindaraju. “Minimizing electrodes for effective brain computer interface”. In: *Biomedical Signal Processing and Control* 63 (2021), p. 102201.

[62] Daniel Kahneman. *Attention and effort*. 1973.

[63] Siddharth Karkare, Goutam Saha, and Joydeep Bhattacharya. “Investigating long-range correlation properties in EEG during complex cognitive tasks”. In: *Chaos, Solitons & Fractals* 42.4 (2009), pp. 2067–2073.

[64] Alexandra P Key et al. “Feasibility of using auditory event-related potentials to investigate learning and memory in nonverbal individuals with Angelman syndrome”. In: *Brain and Cognition* 128 (2018), pp. 73–79.

[65] Kyung Hwan Kim, Seok Won Bang, and Sang Ryong Kim. “Emotion recognition system using short-term monitoring of physiological signals”. In: *Medical and Biological Engineering and Computing* 42 (2004), pp. 419–427.

[66] Min-Ki Kim et al. “A review on the computational methods for emotional state estimation from the human EEG”. In: *Computational and Mathematical Methods in Medicine* 2013.1 (2013), p. 573734.

[67] Wayne K Kirchner. “Age differences in short-term retention of rapidly changing information.” In: *Journal of Experimental Psychology* 55.4 (1958), p. 352.

[68] Johanna Kissler and Cornelia Herbert. “Emotion, Etmnooi, or Emitoon?–Faster lexical access to emotional than to neutral words during reading”. In: *Biological Psychology* 92.3 (2013), pp. 464–479.

[69] Gennadij G Knyazev and Helena R Slobodskaya. “Personality trait of behavioral inhibition is associated with oscillatory systems reciprocal relationships”. In: *International Journal of Psychophysiology* 48.3 (2003), pp. 247–261.

[70] Nicola König et al. “Neural processing of cognitive control in an emotionally neutral context in anxiety patients”. In: *Brain Sciences* 11.5 (2021), p. 543.

[71] Christian A Kothe and Scott Makeig. “Estimation of task workload from EEG data: new and current tools and perspectives”. In: *2011 Annual International Conference of the IEEE Engineering in Medicine and Biology Society*. IEEE. 2011, pp. 6547–6551.

[72] Nitendra Kumar, Khursheed Alam, and Abul Hasan Siddiqi. “Wavelet Transform for Classification of EEG Signal using SVM and ANN”. In: *Biomedical and Pharmacology Journal* 10.4 (2017), pp. 2061–2069.

[73] Zirui Lan et al. “Real-time EEG-based emotion monitoring using stable features”. In: *The Visual Computer* 32 (2016), pp. 347–358.

[74] Peter J Lang, Margaret M Bradley, Bruce N Cuthbert, et al. “International affective picture system (IAPS): Technical manual and affective ratings”. In: *NIMH Center for the Study of Emotion and Attention* 1.39-58 (1997), p. 3.

[75] Peter J Lang, Margaret M Bradley, and Bruce N Cuthbert. “Motivated attention: Affect, activation, and action”. In: *Attention and Orienting*. Psychology Press, 2013, pp. 97–135.

[76] You-Yun Lee and Shulan Hsieh. "Classifying different emotional states by means of EEG-based functional connectivity patterns". In: *PloS One* 9.4 (2014), e95415.

[77] Jinpeng Li, Zhaoxiang Zhang, and Huiguang He. "Implementation of EEG emotion recognition system based on hierarchical convolutional neural networks". In: *Advances in Brain Inspired Cognitive Systems: 8th International Conference, BICS 2016, Beijing, China, November 28-30, 2016, Proceedings 8*. Springer. 2016, pp. 22–33.

[78] Mu Li and Bao-Liang Lu. "Emotion classification based on gamma-band EEG". In: *2009 Annual International Conference of the IEEE Engineering in Medicine and Biology Society*. ieee. 2009, pp. 1223–1226.

[79] Peiyang Li et al. "EEG based emotion recognition by combining functional connectivity network and local activations". In: *IEEE Transactions on Biomedical Engineering* 66.10 (2019), pp. 2869–2881.

[80] Xiang Li et al. "EEG based emotion recognition: A tutorial and review". In: *ACM Computing Surveys* 55.4 (2022), pp. 1–57.

[81] Cheng-Jian Lin and Ming-Hua Hsieh. "Classification of mental task from EEG data using neural networks based on particle swarm optimization". In: *Neurocomputing* 72.4-6 (2009), pp. 1121–1130.

[82] Yi-Hung Liu et al. "Emotion recognition from single-trial EEG based on kernel Fisher's emotion pattern and imbalanced quasiconformal kernel support vector machine". In: *Sensors* 14.8 (2014), pp. 13361–13388.

[83] Junxiu Liu et al. "EEG-based emotion classification using a deep neural network and sparse autoencoder". In: *Frontiers in Systems Neuroscience* 14 (2020), p. 43.

[84] Yisi Liu, Olga Sourina, and Minh Khoa Nguyen. "Real-time EEG-based emotion recognition and its applications". In: *Transactions on Computational Science XII: Special Issue on Cyberworlds* (2011), pp. 256–277.

[85] Steven J Luck. *An Introduction to the Event-Related Potential Technique*. MIT press, 2014.

[86] Ajay Kumar Maddirala and Kalyana C Veluvolu. "Eye-blink artifact removal from single channel EEG with k-means and SSA". In: *Scientific Reports* 11.1 (2021), p. 11043.

[87] Elisa Magosso et al. "EEG alpha power is modulated by attentional changes during cognitive tasks and virtual reality immersion". In: *Computational Intelligence and Neuroscience* 2019.1 (2019), p. 7051079.

[88] Neta B Maimon et al. "Single-channel EEG features during n-back task correlate with working memory load". In: *ArXiv preprint ArXiv:2008.04987* (2020).

[89] Scott Makeig et al. "Evolving signal processing for brain–computer interfaces". In: *Proceedings of the IEEE* 100.Special Centennial Issue (2012), pp. 1567–1584.

[90] Mathilde Ménoret et al. "Evaluating graph signal processing for neuroimaging through classification and dimensionality reduction". In: *2017 IEEE Global Conference on Signal and Information Processing (GlobalSIP)*. IEEE. 2017, pp. 618–622.

[91] Ivana Milovanovic et al. "Simultaneous and independent control of a brain-computer interface and contralateral limb movement". In: *Brain-Computer Interfaces* 2.4 (2015), pp. 174–185.

[92] Zeynab Mohammadi, Javad Frounchi, and Mahmood Amiri. "Wavelet-based emotion recognition system using EEG signal". In: *Neural Computing and Applications* 28 (2017), pp. 1985–1990.

[93] David Morrison et al. "Exploring the raison d'etre behind metric selection in network analysis: A systematic review". In: *Applied Network Science* 7.1 (2022), p. 50.

[94] Gernot R Müller-Putz, René Riedl, Selina C Wriessnegger, et al. "Electroencephalography (EEG) as a research tool in the information systems discipline: Foundations, measurement, and applications". In: *Communications of the Association for Information Systems* 37.1 (2015), p. 46.

[95] Verónica Nácher et al. “Coherent delta-band oscillations between cortical areas correlate with decision making”. In: *Proceedings of the National Academy of Sciences* 110.37 (2013), pp. 15085–15090.

[96] Abeer Al-Nafjan. “Feature selection of EEG signals in neuromarketing”. In: *PeerJ Computer Science* 8 (2022), e944.

[97] Irina-Emilia Nicolae. “Advanced EEG signal processing with applications in brain-computer interfaces: evaluating user focused paradigms for the purpose of enhancing brain-computer interaction”. PhD thesis. Dissertation, Berlin, Technische Universität Berlin, 2018, 2019.

[98] Irina-Emilia Nicolae, Laura Acqualagna, and Benjamin Blankertz. “Assessing the depth of cognitive processing as the basis for potential user-state adaptation”. In: *Frontiers in neuroscience* 11 (2017), p. 548.

[99] Irina-Emilia Nicolae, Laura Acqualagna, and Benjamin Blankertz. “Neural indicators of the depth of cognitive processing for user-adaptive neurotechnological applications”. In: *2015 37th Annual International Conference of the IEEE Engineering in Medicine and Biology Society (EMBC)*. IEEE. 2015, pp. 1484–1487.

[100] Irina-Emilia Nicolae, Laura Acqualagna, and Georgeta-Mihaela Neagu. “Enhanced Classification Methods for the Depth of Cognitive Processing Depicted in Neural Signals”. In: *Universit Politehnica of Bucharest Scientific Bulletin Series C-Electrical Engineering and Computer Science* 80.1 (2018), pp. 135–146.

[101] Jonas K Olofsson et al. “Affective picture processing: an integrative review of ERP findings”. In: *Biological Psychology* 77.3 (2008), pp. 247–265.

[102] Jukka-Pekka Onnela et al. “Intensity and coherence of motifs in weighted complex networks”. In: *Physical Review E—Statistical, Nonlinear, and Soft Matter Physics* 71.6 (2005), p. 065103.

[103] Antonio Ortega et al. “Graph signal processing: Overview, challenges, and applications”. In: *Proceedings of the IEEE* 106.5 (2018), pp. 808–828.

[104] Mirka Pesonen, Heikki Hämäläinen, and Christina M Krause. “Brain oscillatory 4–30 Hz responses during a visual n-back memory task with varying memory load”. In: *Brain Research* 1138 (2007), pp. 171–177.

[105] Panagiotis C Petrantonakis and Leontios J Hadjileontiadis. “Emotion recognition from brain signals using hybrid adaptive filtering and higher order crossings analysis”. In: *IEEE Transactions on Affective Computing* 1.2 (2010), pp. 81–97.

[106] Gert Pfurtscheller et al. “Walking from thought”. In: *Brain Research* 1071.1 (2006), pp. 145–152.

[107] Nora Preuss et al. “Inconsistency and social decision making in patients with Borderline Personality Disorder”. In: *Psychiatry Research* 243 (2016), pp. 115–122.

[108] Yu Qin et al. “Classifying four-category visual objects using multiple ERP components in single-trial ERP”. In: *Cognitive Neurodynamics* 10 (2016), pp. 275–285.

[109] Majid Roshanaei et al. “EEG-based functional and effective connectivity patterns during emotional episodes using graph theoretical analysis”. In: *Scientific Reports* 15.1 (2025), p. 2174.

[110] N Rotem-Kohavi, TF Oberlander, and N Virji-Babul. “Infants and adults have similar regional functional brain organization for the perception of emotions”. In: *Neuroscience Letters* 650 (2017), pp. 118–125.

[111] Mikail Rubinov and Olaf Sporns. “Complex network measures of brain connectivity: uses and interpretations”. In: *Neuroimage* 52.3 (2010), pp. 1059–1069.

[112] ME Saab and Jean Gotman. “A system to detect the onset of epileptic seizures in scalp EEG”. In: *Clinical Neurophysiology* 116.2 (2005), pp. 427–442.

[113] Dean Sabatinelli et al. “Parallel amygdala and inferotemporal activation reflect emotional intensity and fear relevance”. In: *Neuroimage* 24.4 (2005), pp. 1265–1270.

[114] Vangelis Sakkalis et al. "Time-significant wavelet coherence for the evaluation of schizophrenic brain activity using a graph theory approach". In: *2006 International Conference of the IEEE Engineering in Medicine and Biology Society*. IEEE. 2006, pp. 4265–4268.

[115] Yolanda R Schlumpf et al. "Functional connectivity changes in the delta frequency band following trauma treatment in complex trauma and dissociative disorder patients". In: *Frontiers in Psychiatry* 13 (2022), p. 889560.

[116] Eike A Schmidt et al. "Assessing drivers' vigilance state during monotonous driving". In: *Driving Assessment Conference*. Vol. 4. 2007. University of Iowa. 2007.

[117] Li-Chen Shi, Ying-Ying Jiao, and Bao-Liang Lu. "Differential entropy feature for EEG-based vigilance estimation". In: *2013 35th Annual International Conference of the IEEE Engineering in Medicine and Biology Society (EMBC)*. IEEE. 2013, pp. 6627–6630.

[118] Li-Chen Shi and Bao-Liang Lu. "EEG-based vigilance estimation using extreme learning machines". In: *Neurocomputing* 102 (2013), pp. 135–143.

[119] Yajing Si et al. "Predicting individual decision-making responses based on single-trial EEG". In: *NeuroImage* 206 (2020), p. 116333.

[120] M Memarian Sorkhabi. "Emotion detection from EEG signals with continuous wavelet analyzing". In: *Am. J. Comput. Res. Repos* 2.4 (2014), pp. 66–70.

[121] Matteo Spezialetti, Giuseppe Placidi, and Silvia Rossi. "Emotion recognition for human-robot interaction: Recent advances and future perspectives". In: *Frontiers in Robotics and AI* 7 (2020), p. 532279.

[122] Cornelis J Stam and Jaap C Reijneveld. "Graph theoretical analysis of complex networks in the brain". In: *Nonlinear Biomedical Physics* 1 (2007), pp. 1–19.

[123] Carlos Alberto Stefano Filho, Romis Attux, and Gabriela Castellano. "Can graph metrics be used for EEG-BCIs based on hand motor imagery?" In: *Biomedical Signal Processing and Control* 40 (2018), pp. 359–365.

[124] Andrew X Stewart, Antje Nuthmann, and Guido Sanguinetti. "Single-trial classification of EEG in a visual object task using ICA and machine learning". In: *Journal of Neuroscience Methods* 228 (2014), pp. 1–14.

[125] Sirko Straube and Manfred Fahle. "The electrophysiological correlate of saliency: Evidence from a figure-detection task". In: *Brain Research* 1307 (2010), pp. 89–102.

[126] Jipu Su et al. "Subject-independent eeg emotion recognition based on genetically optimized projection dictionary pair learning". In: *Brain Sciences* 13.7 (2023), p. 977.

[127] Cheng Tang et al. "EEG-based emotion recognition via fast and robust feature smoothing". In: *Brain Informatics: International Conference, BI 2017, Beijing, China, November 16-18, 2017, Proceedings*. Springer. 2017, pp. 83–92.

[128] Zhichuan Tang, Chao Li, and Shouqian Sun. "Single-trial EEG classification of motor imagery using deep convolutional neural networks". In: *Optik* 130 (2017), pp. 11–18.

[129] S Thejaswini et al. "An algorithm to detect emotion states and stress levels using EEG signals". In: *International Journal of Latest Research in Engineering and Technology (IJLRET)* (2017), pp. 5–12.

[130] Edgar P Torres et al. "EEG-based BCI emotion recognition: A survey". In: *Sensors* 20.18 (2020), p. 5083.

[131] Arturo Torres-Herraez, Thomas C Watson, and Laure Rondi-Reig. "Delta oscillations coordinate intracerebellar and cerebello-hippocampal network dynamics during sleep". In: *Journal of Neuroscience* 42.11 (2022), pp. 2268–2281.

[132] Nugraha P Utama et al. "Single-trial EEG data to classify type and intensity of facial emotion from P100 and N170". In: *2009 International Joint Conference on Neural Networks*. IEEE. 2009, pp. 3156–3163.

[133] Martijn P Van Den Heuvel and Hilleke E Hulshoff Pol. "Exploring the brain network: a review on resting-state fMRI functional connectivity". In: *European Neuropsychopharmacology* 20.8 (2010), pp. 519–534.

[134] B Ph Van Milligen et al. "Wavelet bicoherence: a new turbulence analysis tool". In: *Physics of Plasmas* 2.8 (1995), pp. 3017–3032.

[135] Bastian Venthur et al. "Novel applications of BCI technology: psychophysiological optimization of working conditions in industry". In: *2010 IEEE International Conference on Systems, Man and Cybernetics*. IEEE. 2010, pp. 417–421.

[136] Fabrizio de Vico Fallani et al. "Graph analysis of functional brain networks: practical issues in translational neuroscience". In: *Philosophical Transactions of the Royal Society B: Biological Sciences* 369.1653 (2014), p. 20130521.

[137] Maria Viqueira, Begona Garcia Zapirain, and Amaia Mendez. "Wavelet transform for the analysis of EEG signals in patients with oral communications problems". In: *2011 IEEE International Symposium on Signal Processing and Information Technology (ISSPIT)*. IEEE. 2011, pp. 140–143.

[138] Changming Wang et al. "Combining features from ERP components in single-trial EEG for discriminating four-category visual objects". In: *Journal of Neural Engineering* 9.5 (2012), p. 056013.

[139] Guangrong Wang et al. "Medial frontal negativity reflects advantageous inequality aversion of proposers in the ultimatum game: An ERP study". In: *Brain Research* 1639 (2016), pp. 38–46.

[140] Shouyi Wang, Jacek Gwizdka, and W Art Chaovalitwongse. "Using wireless EEG signals to assess memory workload in the $n$-back task". In: *IEEE Transactions on Human-Machine Systems* 46.3 (2015), pp. 424–435.

[141] Xiao-Wei Wang, Dan Nie, and Bao-Liang Lu. "Emotional state classification from EEG data using machine learning approach". In: *Neurocomputing* 129 (2014), pp. 94–106.

[142] Zhongmin Wang, Yue Tong, and Xia Heng. "Phase-locking value based graph convolutional neural networks for emotion recognition". In: *IEEE Access* 7 (2019), pp. 93711–93722.

[143] Duncan J Watts and Steven H Strogatz. "Collective dynamics of 'small-world'networks". In: *Nature* 393.6684 (1998), pp. 440–442.

[144] Stefan Wiens, Anders Sand, and Jonas K Olofsson. "Nonemotional features suppress early and enhance late emotional electrocortical responses to negative pictures". In: *Biological Psychology* 86.1 (2011), pp. 83–89.

[145] Irene Winkler, Stefan Haufe, and Michael Tangermann. "Automatic classification of artifactual ICA-components for artifact removal in EEG signals". In: *Behavioral and Brain Functions* 7 (2011), pp. 1–15.

[146] Xun Wu, Wei-Long Zheng, and Bao-Liang Lu. "Identifying functional brain connectivity patterns for EEG-based emotion recognition". In: *2019 9th International IEEE/EMBS Conference on Neural Engineering (NER)*. IEEE. 2019, pp. 235–238.

[147] Xun Wu et al. "Investigating EEG-based functional connectivity patterns for multimodal emotion recognition". In: *Journal of Neural Engineering* 19.1 (2022), p. 016012.

[148] Vasileios-Rafail Xefteris et al. "Graph theoretical analysis of eeg functional connectivity patterns and fusion with physiological signals for emotion recognition". In: *Sensors* 22.21 (2022), p. 8198.

[149] Yusuke Yokota and Yasushi Naruse. "Phase coherence of auditory steady-state response reflects the amount of cognitive workload in a modified N-back task". In: *Neuroscience Research* 100 (2015), pp. 39–45.

[150] Thorsten O Zander et al. "Enhancing human-computer interaction with input from active and passive brain-computer interfaces". In: *Brain-Computer Interfaces: Applying Our Minds to Human-Computer Interaction* (2010), pp. 181–199.

[151] Jianhai Zhang et al. “ReliefF-based EEG sensor selection methods for emotion recognition”. In: *Sensors* 16.10 (2016), p. 1558.

[152] Zelun Tony Zhang et al. “Measuring the effect of mental workload and explanations on appropriate AI reliance using EEG”. In: *Behaviour & Information Technology* (2024), pp. 1–19.

[153] Jindi Zhao et al. “Auditory event-related potentials based on name stimuli: A pilot study”. In: *Frontiers in Neuroscience* 16 (2022), p. 808897.

[154] Yifan Zhao et al. “A wavelet-based correlation analysis framework to study cerebromuscular activity in essential tremor”. In: *Complexity* 2018.1 (2018), p. 7269494.

[155] Wei-Long Zheng and Bao-Liang Lu. “Investigating critical frequency bands and channels for EEG-based emotion recognition with deep neural networks”. In: *IEEE Transactions on Autonomous Mental Development* 7.3 (2015), pp. 162–175.

[156] Peixiang Zhong, Di Wang, and Chunyan Miao. “EEG-based emotion recognition using regularized graph neural networks”. In: *IEEE Transactions on Affective Computing* 13.3 (2020), pp. 1290–1301.

[157] Guohun Zhu et al. “Cognitive load during multitasking can be accurately assessed based on single channel electroencephalography using graph methods”. In: *IEEE Access* 9 (2021), pp. 33102–33109.